Phonon-Drag Thermomagnetic Effects in *n*-Type Germanium. I. General Survey

C. HERRING, T. H. GEBALLE, AND J. E. KUNZLER
Bell Telephone Laboratories, Murray Hill, New Jersey
(Received March 3, 1958)

In a magnetic field **H** and a thermal gradient ∇T, a conductor develops a Nernst field $-B\mathbf{H}\times\nabla T$ and its thermoelectric power Q depends on **H**. These two effects have been measured for a number of single-crystal six-armed samples of high-purity *n*-type germanium, with various orientations, at fields up to 18 000 gauss and at a number of temperatures from the liquid-hydrogen range to the onset of intrinsic conduction; the most detailed measurements were made near liquid air temperature. Both the Nernst coefficient B and the quantity $\Delta Q=Q(\mathbf{H})-Q(0)$ are compounded additively out of terms arising from diffusion of the electrons and terms arising from their anisotropic scattering by the phonons moving from hot to cold. The latter "phonon-drag" terms are strongly predominant at low temperatures. They give rise to a positive contribution B_p to the low-field B which outweighs the negative electron-diffusion contribution for $T<175°$K, and which can be expressed in terms of Hall mobility μ_H and phonon-drag thermoelectric power Q_p by $B_p=\zeta_p|Q_p|\mu_H/c$ with $\zeta_p\approx0.25$ over most of the range. Theoretically and experimentally, $BH\to0$ as $H\to\infty$. As expected, $\Delta Q(\mathbf{H})$ resembles the magnetoresistance both in its anisotropy and in its variation with **H**. All the results are understandable theoretically in terms of a model which assigns to each ellipsoidal energy shell in crystal-momentum space an anisotropic phonon-drag Peltier tensor with principal components $\Pi_{p\parallel}$ in the high-mass direction, $\Pi_{p\perp}$ in the low-mass direction. The data show that $\Pi_{p\parallel}/\Pi_{p\perp}\gg1$ but $<$ the mass-relaxation-time anisotropy $m_\parallel{}^*\tau_\perp/m_\perp{}^*\tau_\parallel\approx17$. The effective average of $\Pi_{p\parallel}$ and $\Pi_{p\perp}$ increases slightly with decreasing energy of the shell, as it should if the relaxation times of the phonons vary with wave number q at a rate between q^{-1} and q^{-2}. A more quantitative analysis is possible and will be given in a forthcoming paper.

1. INTRODUCTION

IT was discovered a few years ago[1–3] that the thermoelectric powers of semiconductors are often enormously augmented at low temperatures by what has come to be known as the phonon-drag effect, a pushing of the charge carriers from hot to cold by the asymmetrical distribution of phonon motions which the thermal gradient produces. The effect is proportional to the strength of the electron-phonon coupling and to the relaxation time for randomization of the motions of the long-wavelength phonons with which the carriers interact. It therefore provides an opportunity to learn things about electron-phonon interactions which are not revealed by the study of purely electrical transport, and to get information on phonon-phonon interactions in a region of the vibrational spectrum different from that which determines the thermal conductivity.

Although study of the Seebeck effect has already yielded useful insight into these topics,[3,4] one would like to get more detailed and quantitative information. In this present paper and its sequel[5] we shall show that such information can be obtained from measurements of the transverse emf in a magnetic field and a thermal gradient, and of the change of thermoelectric power in a magnetic field. The many orientations and field strengths which one can use for such measurements provide a great wealth of data. These data satisfy fairly accurately not only the relations required by the macroscopic symmetry of the crystal, but also several further identities predicted by a transport theory based on approximations previously used for conduction and galvanomagnetic effects.[6] In addition, one can obtain, usually by several independent means, values of a number of constants relating to the anisotropy of electron-phonon interactions[7] and the magnitudes and frequency dependences of the relaxation times of the phonons. Leaving for future publications the task of comparing these results in detail with the predictions of deformation-potential theory and lattice-vibration theory, we shall be content, here and in our forthcoming paper,[5] to report observations, develop the relevant phenomenological and transport theory, and make a few comments on the general reasonableness of the values obtained for the atomistic parameters.

The most interesting of the conclusions to be drawn from the data will be that the phonons depart appreciably from the "ideal" behavior predicted for phonon-phonon collisions in the limit of low frequencies. This departure has already been foreshadowed[3,8] by the results of experiments[3,8,9] on the effect of the diameter of the specimen on the thermal conductivity and thermoelectric power of germanium at temperatures up to that of liquid air.

A few words are in order regarding the relationship of the present study to other thermomagnetic measurements in the literature, and our reasons for choosing, as the first object for our detailed study, *n*-type germanium of high purity and the range of temperatures

[1] H. P. R. Frederikse, Phys. Rev. **91**, 491 (1953); **92**, 248 (1953).
[2] T. H. Geballe, Phys. Rev. **92**, 857 (1953); T. H. Geballe and G. W. Hull, Phys. Rev. **84**, 1134 (1954).
[3] A review of experiment and theory on phonon-drag effects has been given by C. Herring, in *Halbleiterprobleme*, edited by W. Schottky, (Friedrich Vieweg und Sohn, Braunschweig, 1958), Vol. 4.
[4] C. Herring, Phys. Rev. **96**, 1163 (1954).
[5] Herring, Geballe, and Kunzler (to be published).
[6] C. Herring and E. Vogt, Phys. Rev. **101**, 944 (1956).
[7] C. Herring, Phys. Rev. **95**, 954 (1954).
[8] T. H. Geballe and C. Herring (to be published).
[9] T. H. Geballe and G. W. Hull, *Conférence de Physique des Basses Temperatures* (Union Internationale de Physique Pure et Appliquée—Institut International du Froid, 1956), p. 460.

near that of liquid air. The emf transverse to $\mathbf{H}$ and to ∇T, when these vectors are not parallel, is variously known as the "Nernst" or the "transverse Nernst-Ettingshausen" field; we shall use the shorter term. The modification ΔQ which a magnetic field produces in the thermoelectric power has been termed the "longitudinal Nernst-Ettingshausen effect" or the "magneto-Seebeck effect"; we shall call it simply the "ΔQ effect." Most previous experimental studies[10] of these effects in semiconductors have been at temperatures above the range where phonon drag is important; the interesting effects which theory[11,12] associates with the competition of electrons and holes in intrinsic conduction have received more attention. We have reported[3,13] preliminary measurements of the Nernst effect for n- and p-type germanium in the region (10°–175°K) where phonon-drag effects are predominant, and of the ΔQ effect for n-type germanium. Steele[14] has also reported measurements of the latter quantity at 78°K. More recently, Mochan, Obraztsov, and Krylova[15] have published independent measurements of the Nernst effect in p-type germanium down to liquid air temperature which strikingly resemble ours. Most of the theoretical literature[16,17] has dealt only with the electron-diffusion mechanism of thermal emf's, but recently the probable importance of phonon drag has been pointed out,[12] and elementary discussions of it have been given.[3,18] Except for reference 3, all treatments have assumed an isotropic band structure.

From this perspective it is clear that the next step is a careful quantitative study of phonon-drag thermomagnetic effects. Since these depend on everything that affects the conduction process and on other details of electron-phonon and phonon-phonon interactions besides, the proper place to begin the decipherment is with a material for which as much as possible is known about the scattering laws and transport statistics of the electronic carriers. For n-type germanium both transport theory[6,19,20] and deformation-potential theory[6] are well-advanced and successful. We have therefore concentrated on this material, in the temperature range low enough for phonon drag to be of major importance, but high enough for impurity scattering in the best specimens to be slight.

The full analysis of the thermomagnetic data to be presented naturally requires rather detailed theoretical derivations and the experimental and theoretical tracking down of many side issues. To avoid obscuring the main features of the phenomena by the mass of detail, we have selected to present in this first paper the basic ideas of the theory, the central experimental results, and, accepting these at face value, the qualitative conclusions which can be drawn with little or no mathematics. These conclusions are enumerated and italicized in Sec. 4. In a subsequent paper detailed formulas for the various effects will be derived and fitted to the data, with allowance, when necessary, for various minor perturbing influences.

2. BASIC THEORETICAL CONCEPTS

Definitions and Consequences of Crystal Symmetry

In a conducting medium in isothermal equilibrium, the Fermi level or electrochemical potential ϵ_F of the electrons is everywhere constant. If the temperature T varies with position, thermoelectric emf's will be set up; if the medium is homogeneous and ∇T is constant these can be compensated, at least to the first order in ∇T, by a suitable electrostatic field.[21] We can therefore define a thermoelectric-power tensor $\mathbf{Q}$ by

$$\nabla(\epsilon_F/e)=\mathbf{Q}\cdot\nabla T \quad \text{when the current } \mathbf{j}=0. \qquad (1)$$

For a medium of cubic symmetry, $\mathbf{Q}$ is a multiple of the unit tensor in the absence of a magnetic field, but in the presence of such a field $\mathbf{H}$ it becomes anisotropic. In particular, it acquires an antisymmetric part, which gives rise to an emf normal to ∇T and to $\mathbf{H}$. The Nernst coefficient B is usually defined by writing the transverse field $\mathbf{E}_N$ (for $\mathbf{j}=0$) in the form

$$\mathbf{E}_N=-B\mathbf{H}\times\nabla T. \qquad (2)$$

(This definition gives the so-called "isothermal" Nernst coefficient, whereas most experimental arrangements

[10] Some of the more recent of these are: Fukuroi, Tanuma, and Tobisawa, Sci. Repts. Research Inst. Tohoku Univ. **A2**, 233 (1950) (Te); I. V. Mochan, J. Tech. Phys. (U.S.S.R.) **25**, 1003 (1955) (Te); E. H. Putley, Proc. Phys. Soc. (London) **B68**, 35 (1955) (PbSe, PbTe); T. V. Krylova and I. V. Mochan, J. Tech. Phys. (U.S.S.R.) **25**, 2119 (1955) (Ge); R. I. Bashirov and I. M. Tsidil'kovski, J. Tech. Phys. (U.S.S.R.) **26**, 2195 (1956) (Ge); I. M. Tsidil'kovski, J. Tech. Phys. (U.S.S.R.) **27**, 12 (1957) (HgSe), **27**, 1744 (1957) (HgTe).

[11] V. A. Johnson and K. Lark-Horovitz, Phys. Rev. **73**, 1257 (1948); R. G. Chambers, Proc. Phys. Soc. (London) **A65**, 903 (1952); Yu. N. Obraztsov, J. Tech. Phys. (U.S.S.R.) **25**, 995 (1955); E. H. Putley, Proc. Phys. Soc. (London) **B68**, 35 (1955).

[12] P. J. Price, Phys. Rev. **102**, 1245 (1956).

[13] C. Herring and T. H. Geballe, Bull. Am. Phys. Soc. Ser. II, **1**, 117 (1956).

[14] M. C. Steele, Bull. Am. Phys. Soc. Ser. II, **1**, 225 (1956).

[15] Mochan, Obraztsov, and Krylova, J. Tech. Phys. (U.S.S.R.) **27**, 242 (1957).

[16] Nernst effect in extrinsic material: M. Bronstein, Physik. Z. Sowjetunion **2**, 28 (1932); B. I. Davydov and I. M. Smushkevich, Progr. Phys. Sci. (U.S.S.R.) **24**, 21 (1940); R. W. Wright, Proc. Phys. Soc. (London) **A64**, 984 (1951); K. B. Tolpygo, Proc. Inst. Physics, Ukrainian S.S.R. **3**, 52 (1952); O. Madelung, Z. Naturforsch. **9a**, 667 (1954); F. G. Bass and I. M. Tsidil'kovski, J. Exptl. Theoret. Phys. (U.S.S.R.) **31**, 672 (1956) [translation: Soviet Phys. JETP **4**, 565 (1957)]; see also references 11 and 12.

[17] Theory of ΔQ: M. Rodot, Compt. rend. **243**, 129 (1956); see also the papers of Tolpygo and of Bass and Tsidil'kovski, reference 16.

[18] V. L. Gurevich and Yu. N. Obraztsov, J. Exptl. Theoret. Phys. (U.S.S.R.) **32**, 390 (1957) [translation: Soviet Phys. JETP **5**, 307 (1957)].

[19] B. Abeles and S. Meiboom, Phys. Rev. **95**, 31 (1954); M. Shibuya, Phys. Rev. **95**, 1385 (1954).

[20] C. Herring, Bell System Tech. J. **32**, 237 (1955).

[21] It can be shown that in an anisotropic medium a temperature distribution with nonconstant ∇T in general leads to circulating currents which cannot be annulled by an electric field satisfying $\nabla\times\mathbf{E}=0$. See, for example, C. Herring, Phys. Rev. **59**, 889 (1941). However, such situations are of no concern to us here.

measure the "adiabatic" coefficient. For high-purity semiconductors, where lattice thermal conduction far outweighs electronic, the difference between the two types of coefficient is completely negligible.) In the low-field limit, the B of a cubic crystal is isotropic, and in general, if ∇T is in the x direction, $\mathbf{H}$ in the z direction,

$$BH=-Q_{yx}. \tag{3}$$

Care is sometimes needed in using relations like (3), in that the symmetry properties of the $\mathbf{Q}$ tensor are not the same as those of the conductivity or resistivity tensor; for example, calculations[5] show that $-Q_{yx}\neq Q_{xy}$ when the z direction is along a twofold symmetry axis. This difference, which is discussed in Appendix A, originates from the fact that whereas the conductivity tensor $\boldsymbol{\sigma}(\mathbf{H})$ is related to $\boldsymbol{\sigma}(-\mathbf{H})$ both by crystal symmetry and by the Onsager relations, only the former relates $\mathbf{Q}(\mathbf{H})$ and $\mathbf{Q}(-\mathbf{H})$, since the Onsager relations connect $\mathbf{Q}$ with the Peltier tensor rather than with itself [see Eq. (5) below]. However, the requirements of crystal symmetry alone, as worked out in Appendix A, suffice to restrict Q_{xy} and Q_{yx} to be odd functions of $\mathbf{H}$, and Q_{xx}, Q_{yy}, and Q_{zz} to be even functions, whenever the z direction ($\|\mathbf{H}$) and the x direction are along symmetry axes of a crystal with holohedral cubic symmetry. This case includes all the experimental arrangements we have used.

When the field H is small, the thermoelectric power in the α direction varies quadratically with H, in a way which for a cubic crystal is describable by three parameters q_b, q_c, q_d analogous to the three magnetoresistance constants,[22] or to the elastic constants:

$$\Delta Q_{\alpha\alpha}\equiv Q_{\alpha\alpha}(\mathbf{H})-Q_{\alpha\alpha}(0)=q_bH^2+q_c(\mathbf{H}\cdot\mathbf{u}^{(\alpha)})^2 +q_d[H_x^2(u_x^{(\alpha)})^2+H_y^2(u_y^{(\alpha)})^2+H_z^2(u_z^{(\alpha)})^2], \tag{4}$$

where $\mathbf{u}^{(\alpha)}$ is the unit vector in the α direction, and the x, y, z axes are the cube-edge directions in the crystal.

Kelvin Relation

Whatever may be the atomic mechanisms responsible for the thermoelectric and thermomagnetic effects, they must always, according to irreversible thermodynamics,[23] satisfy the generalized Kelvin relation

$$Q_{\beta\alpha}(\mathbf{H})=\Pi_{\alpha\beta}(-\mathbf{H})/T, \tag{5}$$

where $\boldsymbol{\Pi}$ is the generalized Peltier tensor defined in terms of the heat flux $\mathbf{F}$ in an *isothermal* conduction process. If $\mathbf{j}$ is the current density and $\mathbf{F}$ is understood as the energy flux when the zero of energy for each electron is at the electrochemical potential ϵ_F, the defining equation is

$$\mathbf{F}=\boldsymbol{\Pi}\cdot\mathbf{j}, \quad (\nabla T=0). \tag{6}$$

As was pointed out long ago by Wagner,[24] the Kelvin relation (5) often greatly simplifies the construction of an atomistic theory of thermoelectric effects, since $\boldsymbol{\Pi}$ can be calculated from the solution of an isothermal transport equation, while the direct calculation of $\mathbf{Q}$ requires simultaneous consideration of electrical and thermal gradients. This advantage is conspicuous in the case of phonon-drag effects[3,4] and in this paper we shall calculate the Nernst and ΔQ effects by calculating the antisymmetrical and symmetrical parts of $\boldsymbol{\Pi}$ and using (5). With this approach, the Nernst coefficient measures the heat flux normal to $\mathbf{j}$ and $\mathbf{H}$, and its ratio to the thermoelectric power measures the difference between the Hall angle of the heat flux and that of the electric current.[12]

The utility of computing $\mathbf{Q}$ from $\boldsymbol{\Pi}$ should not prevent us, of course, from thinking at each stage about what happens physically in a thermal gradient, and we shall point this out qualitatively from time to time. Both the Q and Π problems can be valuable aids to physical insight.

All the equations we have written are based on the assumption that relations such as (1) and (6) are point relations, i.e., that the thermoelectric potential gradient at a point depends on the thermal gradient at the same point. This can fail if ∇T is inhomogeneous[21] or if the medium is inhomogeneous, or if the dimensions of the specimen are comparable with the mean free paths of the phonons whose drag contributes to Q. In such cases a Kelvin relation still holds if it is formulated in terms of the voltages and heat fluxes at specific electrodes, rather than in terms of $\mathbf{Q}$'s and $\boldsymbol{\Pi}$'s of a medium; however, its form is less convenient for treating things like the Nernst effect.[3] This difficulty need not concern us here, as the quantitative correlation of theory and experiment in the present paper will be restricted to a temperature range high enough for the mean free paths of the phonons to be very short compared with the diameters of the specimens.

Electron-Group Concept

We must now turn to atomistic theory. In all kinds of conduction processes, it is a great help to our insight to be able to say, for some given set of driving fields, "the high-energy electrons do this, the low-energy electrons do that," or "electrons of the first valley do this, electrons of the second valley do that," etc. Fortunately, transport processes in a multivalley semiconductor like n-type germanium can be described to a rather high degree of accuracy by a mathematical approximation which corresponds exactly to this instinctive way of thinking. This is what we shall call the "electron-group approximation." Consider the group g of states lying in a particular energy range ϵ to $\epsilon+d\epsilon$ in a particular valley i, i.e., in the neighborhood of the ith one of the four distinct band-edge points of

[22] F. Seitz, Phys. Rev. **79**, 376 (1950); G. L. Pearson and H. Suhl, Phys. Rev. **83**, 768 (1951).

[23] Fieschi, de Groot, and Mazur, Physica **20**, 67 (1954).

[24] C. Wagner, Z. physik. Chem. **B22**, 195 (1933).

the Brillouin zone. Let $\mathbf{j}_g$ be the contribution which the carriers in this group of states make to the current density. For most ordinary conditions each such $\mathbf{j}_g$ is, to a good approximation, determined by the applied fields and the scattering law for group g, independently of the behavior of other such groups.[6] Conduction and galvanomagnetic problems can therefore be solved by the simple prescription: first, determine the $\mathbf{j}_g$'s in the given fields; second, add up to get $\mathbf{j}=\sum_g \mathbf{j}_g$. As the distribution function over any one of these energy-shell groups is to a good approximation determined by its $\mathbf{j}_g$ alone, we can solve other transport problems (e.g., the determination of the Peltier tensor) by evaluating other sums of the form $\sum_g f(\mathbf{j}_g)$.

This convenient way of solving transport problems can be applied not only to multivalley semiconductors, but also, though perhaps with less accuracy, to the calculation of effects arising from the interplay of electrons and holes, of light and heavy holes, etc. Its validity depends on the fulfillment of two assumptions: (i) that it be possible to divide the possible states of the carriers into a number of groups g, in such a way that the distribution function for the states in group g is always very nearly the same for a given value of the current $\mathbf{j}_g$ due to this group, regardless of what combination of electric and magnetic fields or thermal gradients has been used to produce this current; and (ii), that each $\mathbf{j}_g$ be determined by the applied fields in a manner independent of the $\mathbf{j}_{g'}$'s of other groups g'. For the energy-shell groups described in the preceding paragraph, (i) is satisfied to the extent that the distribution function over each shell can be approximated by a linear function of the three components of crystal momentum, since to this approximation the number of degrees of freedom of the possible distributions (three) does not exceed the number of components of $\mathbf{j}_g$. The criterion (ii) is satisfied if all the scattering processes are one-carrier processes which either lead to final states in the same shell or else randomize the velocity.[6,20] In our forthcoming paper[5] we shall give a rough quantitative analysis of the adequacy of the approximations for n-type germanium; the conclusions are quite favorable.

If we adopt the electron-group picture just outlined, the heat flux in an isothermal conduction process is just the sum of the contributions of all the groups of carriers, and the contribution of each group g is a linear function of the components of the current contribution from that group. Thus

$$\mathbf{\Pi}(\mathbf{H})\cdot\mathbf{j}=\sum_g \mathbf{\Pi}_g\cdot\mathbf{j}_g, \tag{7}$$

where the partial Peltier coefficients $\mathbf{\Pi}_g$ are independent of the magnetic field. With $\boldsymbol{\rho}$ the total resistivity tensor and $\boldsymbol{\sigma}_g$ the partial conductivity tensor of group g (both will have antisymmetric parts in a magnetic field), we have therefore

$$\mathbf{\Pi}(\mathbf{H})=\sum_g \mathbf{\Pi}_g\cdot\boldsymbol{\sigma}_g(\mathbf{H})\cdot\boldsymbol{\rho}(\mathbf{H}). \tag{8}$$

Here the dependence of $\boldsymbol{\sigma}_g$ on $\mathbf{H}$ is determined by the transport equation for group g, and of course $\boldsymbol{\rho}=(\sum_g\boldsymbol{\sigma}_g)^{-1}$.

When the groups g are ellipsoidal shells of states in crystal-momentum space, the tensor $\mathbf{\Pi}_g$ must by symmetry be diagonal in the principal-axis system of the valley i to which g belongs. When the valley has an axis of three- or four-fold symmetry, as is the case for n-type germanium and n-type silicon, $\mathbf{\Pi}_g$ has only two principal components, $\Pi_{||}(\epsilon)$ along this axis and $\Pi_\perp(\epsilon)$ normal to it; these depend on the energy of the shell forming group g, but are independent of the valley i, of external fields, and of impurity scattering. The whole theoretical problem of these papers will therefore be to relate the observed thermoelectric and thermomagnetic phenomena to the two functions $\Pi_{||}(\epsilon)$ and $\Pi_\perp(\epsilon)$, and to relate these in turn to deformation potentials and the laws of phonon-phonon scattering.

Separation of Electron-Diffusion and Phonon-Drag Terms

Since the heat flux can be divided unambiguously into energy carried by the electronic carriers and energy carried by the phonon system, it follows that $\Pi_{||}$, $\Pi_\perp$, and all quantities derived from them (Q, B, etc.) can be divided into electronic and phonon-drag parts. At the low carrier concentrations we are concerned with in this paper, these two parts can be computed independently of each other, in the sense that the modification of the phonon distribution by the motion of the carriers is so slight that the scattering law for the carriers remains practically the same as if the phonons were in equilibrium. At high carrier concentrations the motion of the carriers modifies the phonon distribution more seriously; the "saturation effect"[4] reduces the phonon-drag part of the thermoelectric power, and will modify the thermomagnetic effects correspondingly. However, we can still distinguish the parts of $\Pi_{||}$, $\Pi_\perp$, etc., due to electronic and phonon fluxes, even though the electronic part is now modified by the phonon-drag phenomenon. (Because impurity scattering is usually important at high enough carrier concentrations to produce saturation, the latter modification is usually rather slight.[3,25,26])

We shall therefore write, using the subscripts e for electronic and p for phonon-drag,

$$\begin{gathered}\mathbf{\Pi}=\mathbf{\Pi}_e+\mathbf{\Pi}_p,\quad \Pi_{||}=\Pi_{e||}+\Pi_{p||},\quad \Pi_\perp=\Pi_{e\perp}+\Pi_{p\perp},\\ \mathbf{Q}_e\equiv\mathbf{\Pi}_e/T,\quad \mathbf{Q}_p\equiv\mathbf{\Pi}_p/T,\\ B=B_e+B_p,\quad \text{etc.}\end{gathered} \tag{9}$$

Here

$$\Pi_{e||}=\Pi_{e\perp}=-(\epsilon'-\epsilon_F)/e, \tag{10}$$

where ϵ' is the energy of negative electrons in the shell and ϵ_F is the Fermi level. For the phonon-drag part,

[25] B. Goodman, thesis, University of Pennsylvania, 1954 (unpublished).
[26] J. E. Parrott, Proc. Phys. Soc. (London) **B67**, 587 (1954).

however, $\Pi_{p||}$ and $\Pi_{p\perp}$ may be very different, and one can argue that the anisotropy of Π_{pg} will, except under extreme circumstances, resemble that of the effective-mass tensor m^*. For currents $j_{||}$, $j_\perp$ in the different principal directions of a valley involve crystal momenta proportional to $m_{||}{}^*j_{||}$, $m_\perp{}^*j_\perp$, respectively. They therefore feed crystal momenta into the phonon system at rates proportional to $m_{||}{}^*j_{||}/\tau_{||}$, $m_\perp{}^*j_\perp/\tau_\perp$, respectively, where $\tau_{||}$, $\tau_\perp$ are the relaxation times,[6] for acoustic scattering, for currents in the two directions. If the phonons involved in the two cases have comparable relaxation times, as will usually be the case, this means that $\Pi_{p||}/\Pi_{p\perp}$ will be of the order of $m_{||}{}^*\tau_\perp/m_\perp{}^*\tau_{||}$.

Low-Field Nernst Coefficient

As we have remarked in our discussion of the Kelvin relation above, the ratio of the low-field Nernst coefficient B to the thermoelectric power Q measures the difference between the Hall angles of the heat flux $\mathbf{F}$ and the current $\mathbf{j}$ in a weak magnetic field. Different carrier groups give different contributions $\mathbf{F}_g$, $\mathbf{j}_g$, to $\mathbf{F}$ and $\mathbf{j}$, respectively, and one can say crudely that B will be positive if larger-than-average $\mathbf{\Pi}_g$'s correlate with larger-than-average Hall angles among the $\mathbf{j}_g$'s, negative if the reverse. In Appendix B we give a precise expression for B (or B_p or B_e) in the form of a correlation between departures of the tensor $\mathbf{\Pi}_g$'s from their mean and departures of the Hall currents from their mean; a slightly different derivation has been given in reference 3, Eq. (46). Here, however, we shall merely show schematically how this principle works out for B_e and B_p.

Consider first the electronic part B_e. We use (10), noting however that for nondegenerate statistics the major part of (10) involves the distance of the band edge from the Fermi level, a quantity which is the same for all groups g. Now any scalar term of this sort in $\mathbf{\Pi}_g$ contributes to the heat flux $\mathbf{F}=\sum_g \mathbf{\Pi}_g\cdot\mathbf{j}_g$ a term parallel to the total current $\mathbf{j}$, hence nothing to the part of $\mathbf{F}$ perpendicular to $\mathbf{j}$, to which B is related by (3) and (5). So for the calculation of B_e we can replace the ϵ_F in (10) by the band-edge energy or any other arbitrary constant. Let us choose the band-edge energy ϵ_b for simplicity, and set, for each electron group g,

$$\Delta\Pi_{eg}=-(\epsilon-\epsilon_b)/e, \quad \Delta\mathbf{F}_{eg}=\mathbf{F}_{eg}+\mathbf{j}(\epsilon_b-\epsilon_F)/e. \quad (11)$$

For pure acoustic scattering we then have the situation shown in Fig. 1(a), which is schematized to show only two groups, high-energy electrons (1) and low-energy ones (2). The latter have the larger Hall angle, but the former have the larger contribution to $-\Delta\mathbf{F}_e$. Therefore the Hall angle of the heat flow is less than that of the current, and $\mathbf{F}_e$, or $\Delta\mathbf{F}_e$, has a negative component perpendicular to $\mathbf{j}$. This corresponds to the negative B_e which is known to occur for this case.[16] If sufficient impurity scattering is present to make the low-energy electrons have smaller Hall angles than the high-energy ones, B_e becomes >0.

The phonon-drag part B_p of B differs from the electronic in that the $\mathbf{\Pi}_{pg}$'s may be quite anisotropic, in contrast to (10), i.e., $\Pi_{p||}\neq\Pi_{p\perp}$. Therefore two effects contribute to B_p, namely, the variation of the $\mathbf{\Pi}_p$'s with energy, and the interplay of the anisotropy of the $\mathbf{\Pi}_{pg}$'s with that of the partial conductivities σ_g. Moreover, both effects apply to all of $\mathbf{\Pi}_p$, whereas the major contribution to Π_e for nondegenerate material, namely, the difference $(\epsilon_F-\epsilon_b)/e$, was the same for all groups

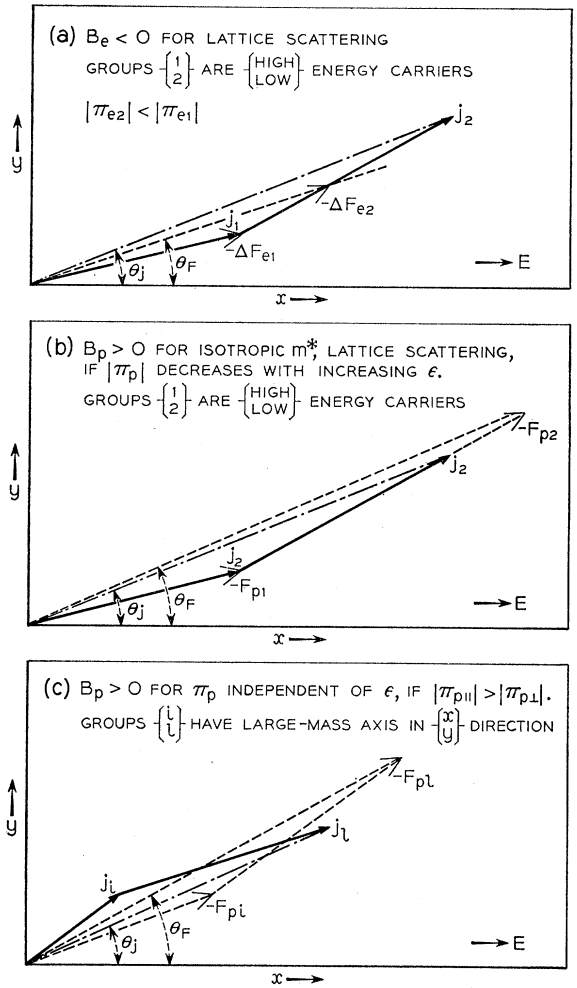

FIG. 1. Schematic behavior of the contributions of two carrier groups to the current density $\mathbf{j}$ (small-headed arrows) and to the heat flux $\mathbf{F}$ (large-headed arrows). For negative carriers $\mathbf{F}$ and $\mathbf{j}$ have opposite signs, but the angles are the same for either sign. The sign of a contribution B_e or B_p to the Nernst coefficient is determined in each case by the sign of the difference $\theta_F-\theta_j$ of the Hall angles. Case (a) depicts the $\Delta\mathbf{F}_e$ vectors, defined by Eq. (11), for carriers of two different energy ranges, and shows how the sign of B_e depends on whether low- or high-energy carriers have the longer relaxation time. Cases (b) and (c) show how the sign of B_p is influenced by the variation of $\mathbf{\Pi}_{pg}$ with energy and by its anisotropy, respectively. The arbitrary scale of the $\mathbf{F}$ vectors relative to the $\mathbf{j}$ vectors has been chosen in the way that seemed most convenient for each case.

TABLE I. Guides to the behavior of the Nernst coefficient and of the change of thermoelectric power with magnetic field. It is assumed that $m_{\parallel}{}^{*}\tau_{\perp}/m_{\perp}{}^{*}\tau_{\parallel}>1$. In the top half of the table the entries not in square brackets apply in the neighborhood of what we believe to be the normal situation for pure n-type Ge.

Thermomagnetic quantity (all >0 in the standard situation)	$-B_e$	B_p	$\Delta\lvert Q_e\rvert$	$\Delta\lvert Q_p\rvert$
Effect of:				
Increasing $\Pi_{p\parallel}/\Pi_{p\perp}$	...	increases	...	increases
Increasing $\Pi_p(\text{low }\epsilon)/\Pi_p(\text{high }\epsilon)$ when $\tau_{\parallel,\perp}(\text{low }\epsilon)>[<]\tau_{\parallel,\perp}(\text{high }\epsilon)$	...	increases [decreases]	...	decreases [increases]
Decreasing $\tau_{\parallel,\perp}(\text{low }\epsilon)/\tau_{\parallel,\perp}(\text{high }\epsilon)$ when $\Pi_p(\text{low }\epsilon)>[<]\Pi_p(\text{high }\epsilon)$	decreases	decreases [increases]	decreases	decreases [increases]
Special value for any $\mathbf{H}$, if:				
$\Pi_{p\parallel}=\Pi_{p\perp}$ and indep. of ϵ	...	0	...	0
$\Pi_{p\parallel,\perp}=\Lambda m_{\parallel,\perp}{}^{*}/\tau_{\parallel,\perp}$, Λ indep. of ϵ	...	$\dfrac{\lvert Q_p(0)\rvert\mu_H(0)}{c}\left[\dfrac{R(\infty)-R(\mathbf{H})}{R(0)}\right]$	...	$\lvert Q_p(0)\rvert\dfrac{\Delta\rho(\mathbf{H})}{\rho(0)}$
$\tau_{\parallel,\perp}$ indep. of ϵ	0	...	0	...

hence did not contribute to B_e. Thus, whereas $|B_e|$ is of the order of μ_H/c times k/e, where μ_H is the Hall mobility, $|B_p|$ may be expected to be of the order of μ_H/c times $|Q_p|$, and hence should become $\gg|B_e|$ when $|Q_p|$ has grown to only a fraction of $|Q_e|$.

The energy effect for B_p is illustrated in Fig. 1(b), which would be representative of B_p in a semiconductor with isotropic effective mass. For such a case, B_p will be >0 if electron groups with large Hall angles (slow electrons, for acoustic scattering) have larger-than-average Π_{pg}'s; this will occur if the relaxation time of the phonons increases sufficiently rapidly with decreasing wave number, since the average wave number for phonons which scatter slow electrons is smaller than for those which scatter fast ones. The anisotropy contribution is illustrated in Fig. 1(c) for a model for which the principal axes of the valleys are along the coordinate directions and for which $m_{\parallel}{}^{*}>m_{\perp}{}^{*}$. Let $\mathbf{E}$ be in the x direction, $\mathbf{H}$ in the z direction. Since for each valley i, $j_x{}^{(i)}\propto 1/m_x{}^{*(i)}$, the major contribution to it will come from those valleys for which the x direction is a small-mass direction, i.e., $\perp$. On the other hand, $j_y{}^{(i)}\propto 1/(m_x{}^{*(i)}m_y{}^{*(i)})$ receives equal contributions from valleys for which x is $\perp$ and $y\parallel$, and those with $x\parallel$, $y\perp$. Now suppose that $|\Pi_{p\parallel}|>|\Pi_{p\perp}|$ and that both are independent of energy, so that each valley can be treated as a unit. Then F_{px}/j_{px} will be determined more by $\Pi_{p\perp}$ and less by $\Pi_{p\parallel}$ than F_{py}/j_{py}. This means that the Hall angle of $\mathbf{F}_p$ will be greater than that of $\mathbf{j}$, so that $B_p>0$. This is the type of anisotropy we expect for silicon. Germanium should behave similarly; the oblique orientations of its valleys do not really modify the conclusions. If for any such model $\Pi_{p\parallel}$ and $\Pi_{p\perp}$ are equal (and independent of energy), the $\mathbf{F}_p$ and $\mathbf{j}$ vectors of each valley will be parallel, their ratio being the same for all valleys; the total $\mathbf{F}_p$ will be parallel to the total $\mathbf{j}$, and B_p will vanish. A negative B_p will result, finally, if for $m_{\parallel}{}^{*}>m_{\perp}{}^{*}$ we have $|\Pi_{p\parallel}|<|\Pi_{p\perp}|$.

The conclusions we have reached are summarized in the columns B_e, B_p of the upper part of Table I; they are given quantitative expression by formulas of our forthcoming paper.[5] It should be noted throughout that for similar band structures and scattering laws the sign of B is the same for electrons as for holes, since both the Hall angles and the Peltier coefficients of the carrier groups reverse sign with change of sign of the carriers.

Vanishing of BH as $H\rightarrow\infty$

As the magnetic field H becomes infinite, the Hall angle of every group of carriers must approach $\pi/2$. If the partial conductivities and Peltier coefficients of the different groups were isotropic, the current contributions $\mathbf{j}_g$ and the heat-flux contributions $\mathbf{F}_g$ would all approach the direction of $\mathbf{E}\times\mathbf{H}$, and so the component of $\mathbf{F}$ normal to $\mathbf{j}$ would go to zero, i.e., $BH\rightarrow 0$. When the groups are anisotropic the different $\mathbf{F}_g$'s do not all approach the same direction; however, one can show, even without using the electron-group approximation, that the total $\mathbf{F}$ approaches parallelism to j. Swanson[27] has shown, in fact, that for given total current $\mathbf{j}$ the distribution function of the carriers must always approach a definite limiting form as $H\rightarrow\infty$, whatever the band structure or the scattering law, provided only that the use of a transport equation in crystal-momentum space remains valid. This limiting distribution function is the same for $-\mathbf{H}$ as for $\mathbf{H}$. Consequently for given $\mathbf{j}$ the heat flux $\mathbf{F}$ will approach a definite limit $\mathbf{F}_\infty$, the same for $\mathbf{H}$ as $-\mathbf{H}$. Therefore if the Nernst voltage BH is defined as that part of the transverse voltage which is odd in $\mathbf{H}$, a definition agreeing with (2) and (3) for all the orientations we shall use, we must have $BH\rightarrow 0$ as $H\rightarrow\infty$. The plot of Nernst voltage against H must thus rise linearly at small H, pass through a maximum, and fall off to a zero asymptote. Figure 9 in Sec. 4 shows that this is indeed the case.

This conclusion does not need to hold when the effects of quantization of the electronic orbits in the magnetic field become important. Whereas transport

[27] J. A. Swanson, Phys. Rev. **99**, 1799 (1955).

theory in a continuous crystal-momentum space predicts a saturation of the magnetoresistance at high fields, calculations for the case where the spacing of the cyclotron levels is $\gg kT$ have shown a continuing change of resistance with H. For acoustic scattering, for example, the resistance parallel to $\mathbf{H}$ is proportional to H,[28,29] and that perpendicular to $\mathbf{H}$ is roughly proportional[30] to H^2. Thus in the transverse case the angle of $\mathbf{j}$ to $\mathbf{E}$ does not in general approach $\pi/2$ as $\mathbf{H}\rightarrow\infty$. Since this angle will have different values for carriers belonging, say, to different valleys, and since the Peltier coefficients of the different valleys will also differ, there is no reason why the angle between the heat flux $\mathbf{F}$ and the current $\mathbf{j}$ should go to zero. However, this angle will normally attain very small values, of the order of a fraction of the minimum value of the ratio ρ/RH of the resistivity in the current direction to the Hall resistivity. In the temperature range of interest to us here, the above reasoning means that as $H\rightarrow\infty$ the minimum value of BH should be less than a percent or so of its maximum value.

Change of Thermoelectric Power with H

This effect can be broken down into the changes ΔQ_e, ΔQ_p, in the electronic and phonon-drag terms, respectively. The symmetry arguments given in Appendix A show that, for all the orientations we shall consider, each of these is an even function of $\mathbf{H}$. Moreover, each must approach a finite saturation value as $H\rightarrow\infty$, as long as the transport equation remains valid, because for a given current the distribution function of the carriers approaches a limiting form; this makes the Peltier heat approach a limiting value.

The value of $|\Delta Q_e|$ cannot become greater than k/e times a factor of order unity, since the magnetic field can only affect the transport term in Q_e, the position of the Fermi level remaining essentially unchanged as long as $kT\gg$ the cyclotron spacing, as we shall assume here. On the other hand, ΔQ_p can become of the same order as Q_p itself. To see this, we note that Π_p is proportional to the rate at which crystal momentum is fed to the phonon system from the charge carriers, and to the mean relaxation time of the phonons.[4] For pure acoustic scattering the rate of transfer of crystal momentum, for given current, is proportional to the force which the external fields have to exert on the carriers to maintain this current. The longitudinal part of this force is due to the electric field only, the magnetic field making no contribution. The electric field required for a given current is proportional to the resistivity. We know that a large magnetic field can sometimes increase the resistivity several fold. A comparable increase in Q_p is thus to be expected, except in the unlikely event that the change in the mean relaxation time of the phonons, due to the altered distribution of their wave numbers, happens to be such as to compensate it.

In our forthcoming paper we shall derive expressions for ΔQ_e and ΔQ_p in terms of the functions $\Pi_{\parallel}(\epsilon)$, $\Pi_{\perp}(\epsilon)$ of the electron-group picture, for both small and large magnetic fields. The effects can be described qualitatively as follows, for the case of nondegenerate statistics and acoustic scattering:

For $H=0$, the current is carried more by the slow electrons than by the fast ones, since the relaxation time τ increases with decreasing energy. As $H\rightarrow\infty$, the distribution of current over the energy groups approaches that which would obtain at $H=0$ if τ were independent of energy. Therefore ΔQ_e, which depends only on the variation of the current contributions with the energies of the groups, will approach a value equal to the difference between the Q_e values for $\tau=$constant and $\tau\propto\epsilon^{-\frac{1}{2}}$. Specifically, Q_e, which is + or − depending on the sign of the carriers, will increase in absolute value, as $H\rightarrow\infty$, by $k/2e=43\ \mu$v/deg.

The value of ΔQ_p is affected both by the just-mentioned change in the relative current contributions of groups of different energy, and by the change in the directions of the currents of the different groups. For acoustic scattering the former effect gives a positive contribution to $\Delta|Q_p|$ if $\Pi_{p\parallel}(\epsilon)$ and $\Pi_p(\epsilon)$ increase with increasing energy, and a negative one if they decrease. As for the directions of the current contributions $\mathbf{j}_g$, these tend to prefer low-mass directions in each valley when $H=0$. If $\mathbf{H}$ is normal to the total current $\mathbf{j}$, the projection of each $\mathbf{j}_g$ normal to $\mathbf{H}$ must as $H\rightarrow\infty$ approach parallelism to $\mathbf{E}\times\mathbf{H}$, hence to $\mathbf{j}$. (Because of the inertial anisotropy, the $\mathbf{j}_g$'s will in general have components along $\mathbf{H}$ of the same order as the normal components; these cancel out on summing on g.) If $\mathbf{H}$ is parallel to $\mathbf{j}$, each $\mathbf{j}_g$ approaches parallelism to $\mathbf{H}$, hence again to $\mathbf{j}$. In either case, therefore, as H increases the Peltier heat is determined more by $\Pi_{\parallel}$ and less by $\Pi_{\perp}$; if $\Pi_{p\parallel}\gg\Pi_{p\perp}$, as we have argued above is to be expected, a positive contribution to $\Delta|Q_p|$ will result.

The same type of reasoning enables us to predict the qualitative effects of impurity and other kinds of

[28] P. N. Argyres and E. N. Adams, Phys. Rev. **104**, 900 (1956).
[29] J. Appel, Z. Naturforsch. **11a**, 892 (1956).
[30] An ingenious approach to the problem of transverse magnetoresistance in high fields has recently been elaborated by M. I. Klinger, J. Exptl. Theoret. Phys. (U.S.S.R.) **31**, 1055 (1956) [translation: Soviet Phys. JETP **4**, 831 (1957)]; M. I. Klinger and P. I. Voronyuk, J. Exptl. Theoret. Phys. (U.S.S.R.) **33**, 77 (1957) [translation: Soviet Phys. JETP **6**, 59 (1958)]. The analysis given in the latter paper really applies, however, only when the ratio of the cyclotron $\hbar\omega_c$ spacing to kT greatly exceeds the square of the ratio $\bar{v}/c$ of the mean electronic velocity to the speed of sound. Under these conditions (millions of gauss for germanium at hydrogen temperatures) the magnetoresistance can again saturate. When $\hbar\omega_c\gg kT$ but $\ll kT(\bar{v}/c)^2$, a simple homology argument based on the ideas of Klinger and Voronyuk shows that the acoustic-scattering magnetoresistance goes almost as H^2.

Note added in proof.—Since this was written, an alternative approach to the problem of transverse magnetoresistance has been given by P. N. Argyres, Phys. Rev. **109**, 1115 (1958), and P. A. Wolff (unpublished). This approach predicts a high-field resistivity proportional to H for acoustic scattering, rather than H^2. The remarks in the text apply for either behavior, the important feature being that the Hall angle does not go to $\pi/2$.

scattering. Ionized-impurity scattering increases $|Q_e|$ at $H=0$, but does not affect the limit of Q_e as $H\to\infty$; thus it decreases $\Delta|Q_e|$, and can even reverse its sign. The energy effect on ΔQ_p is similar; normally a little impurity scattering will make the energy effect less pronounced, and a lot of impurity scattering will reverse it. The anisotropy contribution to ΔQ_p (normally the dominant one) will also be altered by impurity scattering, since it is known that impurity scattering alters the anisotropy of the relaxation time.[31]

The last columns of the top part of Table I summarize the conclusions we have reached.

A Special Case

There is a simple theorem, included of course in the detailed results to be published later,[5] which provides a rough quantitative guide for the interpretation of the data. One can show[6] that in the electron-group approximation each energy-shell group is describable by a relaxation-time tensor $\boldsymbol{\tau}$, with components $\tau_{\parallel}$, $\tau_{\perp}$, and that the magnetoresistance and other static-field transport properties depend only on the tensor $\mathbf{m}^*\boldsymbol{\tau}^{-1}$. If for each such group the partial Peltier tensor Π_{pg} were proportional to the tensor $\mathbf{m}^*\boldsymbol{\tau}^{-1}$, with a factor independent of energy, then the sum $\sum_g \boldsymbol{\Pi}_{pg}\cdot\mathbf{j}_g$ would be proportional to the total force exerted by the external fields on the carriers. In line with what has been said above, this means that $\Delta Q_p/Q_p$ would be exactly equal to the relative resistance change $\Delta\rho/\rho_0$, for arbitrary value of the magnetic field $\mathbf{H}$.

To compute the Nernst coefficient for this special case we merely need, by (3), (5), and the above, to compute the total transverse force exerted on the carriers by the magnetic field and the Hall field. The ratio of $HB_p(\mathbf{H})$ to $Q_p(0)$ is just the ratio of this total force to the longitudinal force exerted by the electric field at $H=0$, and an easy calculation gives

$$B_p(\mathbf{H})=|Q_p(0)|\frac{\mu_H(0)}{c}\left[\frac{R(\infty)-R(\mathbf{H})}{R(0)}\right], \qquad (12)$$

where $R(\mathbf{H})$ is the Hall constant, μ_H the Hall mobility. This equation holds at any $\mathbf{H}$. When $\mathbf{H}$ is in a symmetry direction, R is independent of the direction of the current normal to $\mathbf{H}$, so the B_p of (12) also has circular symmetry about $\mathbf{H}$. For more general models this symmetry is not present when $\mathbf{H}$ is large and along a twofold axis, as is shown by Appendix A and by the calculations of our forthcoming paper.[5]

The bottom half of Table I summarizes the results just derived, together with those for other special cases considered earlier.

The present result is quite distinct from that of Gurevich and Obraztsov,[18] who showed that for the simple model with isotropic effective mass the assumption $\Pi_{pg}\propto\tau$ leads to $B_p(H)\propto\Delta\rho/\rho_0^2$, $Q_p(H)\propto R(H)$. Our result is more useful for n germanium than theirs because the anisotropy of $\boldsymbol{\Pi}_{pg}$ is more important than its variation with energy.

[31] F. S. Ham, Phys. Rev. **100**, 1251 (1955); M. Glicksman, Phys. Rev. **108**, 264 (1957); C. Goldberg, Phys. Rev. **109**, 331 (1958).

Q Approach

So far our discussion of thermomagnetic effects has been entirely in terms of what may be called the Π approach, i.e., calculating $\boldsymbol{\Pi}$ and using (5). This is usually simpler than the direct calculation of $\mathbf{Q}$; however, a few words about the physical processes in a thermal gradient will be helpful to round out the intuitive appeal of the theory.

In the absence of electric and magnetic fields, a thermal gradient will produce a current $\mathbf{j}_g$ in each group of states. By the basic assumption of the electron-group picture the distribution function within group g will be nearly the same as if the identical current $\mathbf{j}_g$ were produced isothermally by an electric field. Thus as far as group g is concerned, any ∇T is equivalent in its effect to some electric field $\mathbf{E}_g$, and we may define a partial thermoelectric power tensor $\mathbf{Q}_g$ for the group by

$$\mathbf{E}_g=-\mathbf{Q}_g\cdot\nabla T. \qquad (13)$$

In the presence of electric and magnetic fields the effects of these and ∇T on the distribution function are additive, to the first order, so that $\mathbf{j}_g$'s in any situation are determined by a transport equation of the usual type—Eq. (13) or (15) of reference 6—but with $\mathbf{E}$ replaced by $\mathbf{E}+\mathbf{E}_g$. The quantities $\mathbf{Q}_g$ are related to the $\boldsymbol{\Pi}_g$'s used earlier in this section by the analog of (5); since they are independent of $\mathbf{H}$, we have simply

$$Q_{g\alpha\beta}=Q_{g\beta\alpha}=\Pi_{g\alpha\beta}/T. \qquad (14)$$

For zero total current the thermoelectric $\mathbf{E}$ balances $\mathbf{E}_g$ on the average, but for some groups g the difference $\mathbf{E}-\mathbf{E}_g$ will point one way, for others a different way. Thus in a thermal gradient there will be counter currents. If the different groups have different ratios of Hall conductivity to longitudinal conductivity, application of a magnetic field will require a transverse electric field to keep the total current zero. Thus all our conclusions on the Nernst effect can be understood from this viewpoint; it is an amusing exercise to verify the other results of this section in a similar way.

3. EXPERIMENTAL PROCEDURE

Objectives

The theoretical considerations just presented make it clear that the objectives for this first detailed study of thermomagnetic effects in n-type germanium should be to check the applicability of the electron-group picture and the theory of the electron-diffusion contributions B_e, ΔQ_e, and then to obtain as much information as possible on the values and energy dependences of the phonon-drag Peltier coefficients

TABLE II. Characteristics of samples used.

Sample No.	Cut from crystal No.	Orientation $[\nabla T, H_{\parallel}]$	Orientation $[H_{\perp}]$	Majority impurity if known	$N_D \times 10^{-13}$, in cm^{-3}	$N_A \times 10^{-13}$, in cm^{-3}
576, 576A	VIII-532	[110]	[001]	Sb	10	1
577	VIII-532	(not simple)		Sb	10	1
591	IV-194	[100]	[001]	As	180	6
594	ZL815B18	[100]	[001]	...	1.6	0.3
595	ZL698B11	[111]	[01$\bar{1}$]	...	$0.3+N_A$	...
596	IV-194	[100]	[001]	As	180	6
601	VIII-532	[100]	[001]	Sb	26	2
603	Z-138A	[110]	[1$\bar{1}$0]	...	2.0	~0.3
604	Z-138A	[100]	[110]	...	2.0	~0.6
606	VIII-129	[100]	[001]	...	1.0	~0.2

$\Pi_{p\parallel}(\epsilon)$, $\Pi_{p\perp}(\epsilon)$ of the different energy shells. Since we did not wish to rely on any existing theory of impurity scattering, we decided to make the measurements both on the purest specimens obtainable and on specimens of slightly lesser purity, in the hope of being able to extrapolate the results to the limit of zero impurity scattering. As was mentioned in the introduction, the main measurements were planned for a temperature high enough for impurity scattering to be slight, but low enough to allow a sizable phonon-drag effect; the region around 90°K was chosen. To check on the electron-diffusion contributions, some measurements were taken up to the temperature of intrinsic conduction; and, to check on boundary-scattering of phonons and orbital quantization, a few measurements were made down to hydrogen temperatures. All quantities were investigated in a number of orientations and at high and low magnetic fields, since the high-field results depend more on the behavior of the $\mathbf{\Pi}_g$'s of high-energy shells, while the low-field results depend on those of low-energy shells. The interpretation of the results depends on the mobility and scattering laws of the electrons, and since there can be variations of as much as 10% in the mobility of high-purity germanium, arrangements were made to take complete Hall and magnetoresistance data for each sample. In most cases this was done in the thermal gradient along with the thermomagnetic data. This means that the low and high magnetic field behavior of the following six properties was investigated: Hall effect, R; Nernst effect, B; transverse ΔQ and magnetoresistance $\Delta\rho$; and longitudinal ΔQ and $\Delta\rho$. To obtain a clear picture of the variation of these quantities with temperature and orientation and of their reproducibility and dependence on purity, the measurements were made at selected temperatures from 14°K to the onset of intrinsic conduction.

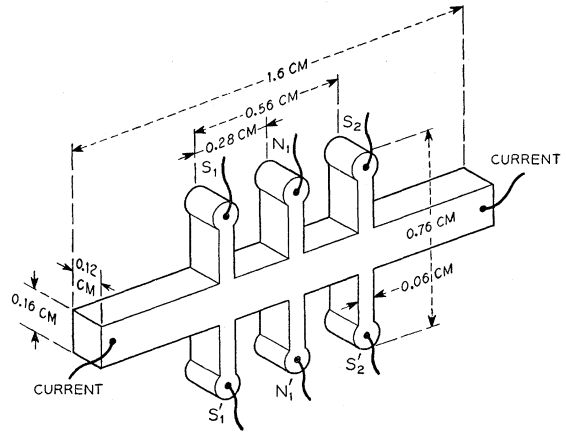

FIG. 2. Six-armed sample showing dimensions and lead wires. The transverse voltages were normally read across N_1N_1' and the longitudinal across S_1S_2. S_1' and S_2' were used with S_1 and S_2 for checking homogeneity.

Samples

The shape and dimensions of the six-armed germanium samples are shown in Fig. 2. They were prepared from high-purity single-crystal germanium by the methods introduced by Pearson and Bond and described previously.[32] A complete list of the samples and their electrical and thermomagnetic properties is given in our forthcoming paper[5]; their orientations, and impurity contents determined from analysis of low-temperature Hall data, are given in Table II. The samples were oriented to within one degree using optical methods, and, in some cases to within a few minutes using an x-ray goniometer modified for that purpose by W. L. Bond. Eight electrical contacts that were of reasonably low resistance and ohmic in character were made to the sample extremities, as indicated in Fig. 2, by alloying 0.008-cm diameter gold wires containing 0.01% antimony. The sample surfaces were sand-blasted with 600-mesh silicon carbide powder. In some cases a "superoxol" etch was subsequently used to investigate surface effects.

Apparatus

During the course of this investigation two different types of experimental apparatus were used. Some of the results were obtained in the more general-purpose thermoelectric apparatus shown in Fig. 3, but most were obtained in the special-purpose apparatus shown in Figs. 4 and 5. The general-purpose apparatus was

[32] P. P. Debye and E. M. Conwell, Phys. Rev. **93**, 693 (1954).

used initially. When it became apparent that both high-field and longitudinal results were important to our program, the special-purpose apparatus was developed. In this section we shall briefly mention some features of each which could not be shown clearly in the figures.

The encapsulated germanium resistance thermometers shown in Fig. 3 have been previously described.[33] These thermometers, along with copper-constantan thermocouples were brought into thermal contact with the arms S_1S_2 (Fig. 2) by means of the liquid gallium wells. These wells were soldered over the electrical contact on the arm and so arranged that the thermometers slid into them as the sample was inserted into the radiation shield. This convenient method of assembly meant that the thermometers did not have to be removed from the apparatus or disconnected electrically while changing samples. This apparatus was useful

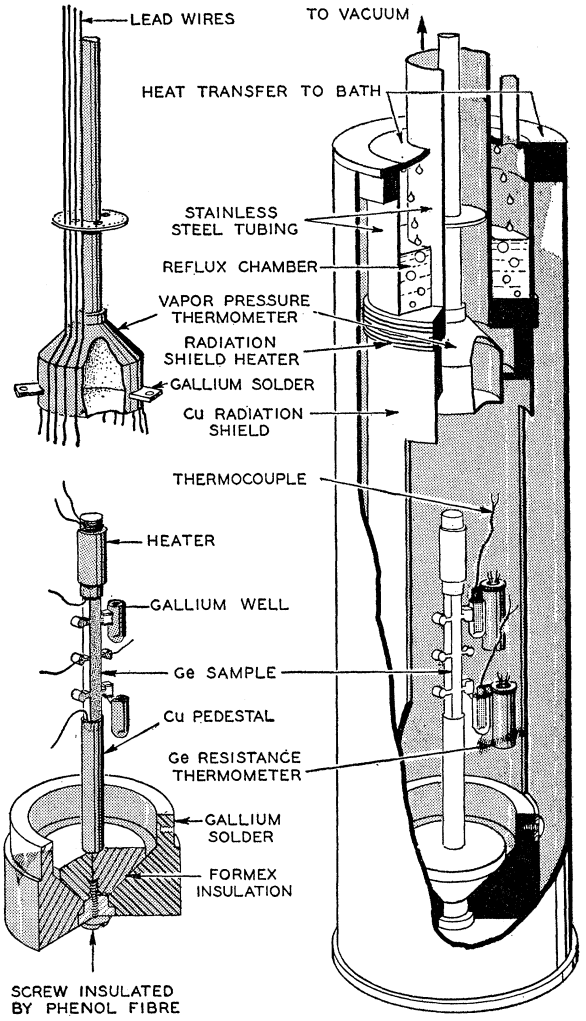

FIG. 3. General purpose apparatus used initially and for obtaining the data of Table II.

[33] Kunzler, Geballe, and Hull, Rev. Sci. Instr. **28**, 96 (1957).

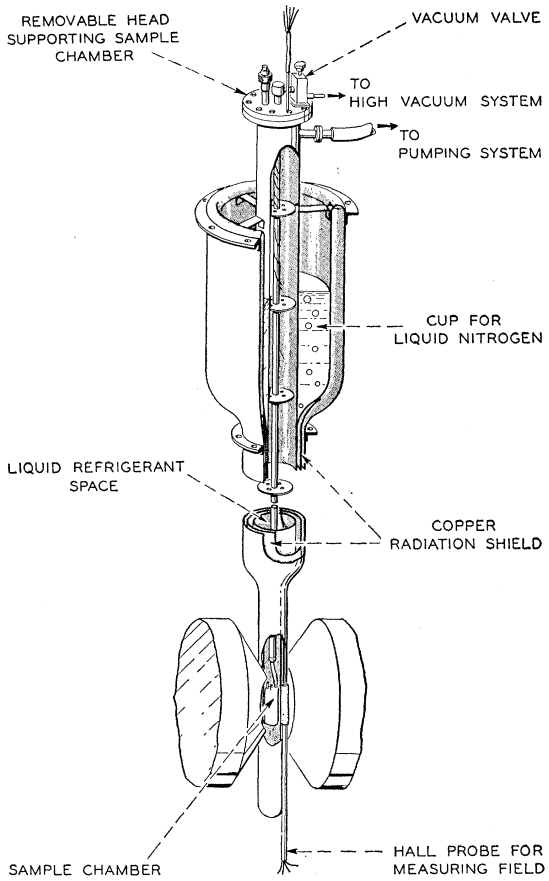

FIG. 4. Specialized apparatus for investigations in longitudinal as well as transverse low and high magnetic fields.

over a continuous temperature range below room temperature with a wide choice of temperature gradient along the sample. The thermal path to the bath through the radiation shield and reflux chamber could be made to vary widely in resistance by controlling the amount of N_2, H_2, or He used as refluxing liquid. The Dewar and an electromagnet capable of producing transverse magnetic fields up to 5000 gauss outside the sample chamber are not shown.

The second, more specialized apparatus is shown in Figs. 4 and 5. The Dewar was centered in a 4.4-cm gap between the pole pieces of the magnet, allowing fields of 18 000 gauss to be reached in both transverse and longitudinal positions. The radial tolerances were close; the 1.5-cm long samples could be fitted inside the 1.9-cm diameter holder which in turn just cleared the lower brass section of the inner wall of the three-walled Dewar. The construction of this Dewar will be described elsewhere.[34] Desired temperatures were reached by using either liquid O_2, N_2, H_2, He or a vacuum in the Dewar and either N_2 or CO_2 in the cup at the top of the Dewar. Furthermore the heat input to the sample

[34] J. E. Kunzler (to be published).

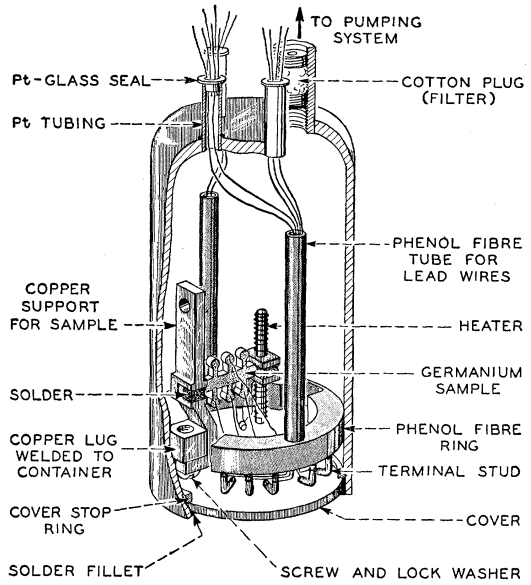

FIG. 5. Enlargment of sample chamber, Fig. 4, showing details of sample mounting and lead wires.

could be widely varied and thus the sample could be kept close to bath temperature or heated considerably above.

The samples were mounted as indicated in Fig. 5 by soldering the heater to one end and the copper link to the other. (The rather intricate shape of the copper link gives the option—not used in this investigation—of putting the axis of the sample in the vertical position without resoldering.) The copper link was placed in thermal contact with the bath by means of a spring-loaded screw. In order to minimize radiation corrections at the higher temperatures and to operate without a permanent vacuum line, the inside of the container was filled with Al_2O_3 powder of $\sim 3\times 10^{-5}$ cm average particle size before soldering on the cover. This served to give good thermal isolation of the sample except through the copper link. The container was pumped out to $\sim 10^{-5}$ mm, checked with a helium leak detector, and sealed off with the high-vacuum valve at the top of the apparatus (Fig. 4).

Measurements

In this section we shall describe briefly how the measurements were made. Since only those measurements involving average temperature and temperature gradient differed significantly in the two types of apparatus, only those will be described separately. In the general-purpose apparatus, Fig. 3, average temperature and temperature gradient were determined by using calibrated encapsulated germanium thermometers below 25°K and copper-constantan thermocouples above.

The sample itself was used for measuring average temperature and temperature gradient in the special-purpose apparatus primarily for the purpose of conserving size. This was possible by making use of both the electrical resistivity-temperature and thermoelectric properties of the germanium sample. The resistivity is a rapidly-varying function of temperature with two extrema between 10 and 300°K.[35] The temperature-resistance curve of each sample was determined simply in a separate experiment and with reasonable care the average sample temperature T could be unambiguously determined from this curve. Temperature differences were found by comparing the Seebeck voltage measured across the arms S_1S_2 to the thermoelectric power Q calculated for T. This Q which one obtains from the sum of Q_e+Q_p could be calculated since Q_p is a property of bulk germanium. Table III lists the best values of Q_p at different temperatures as determined in the general-purpose apparatus. Q_e was calculated from the limiting low-field Hall constant R_0 by using the equation

$$Q_e=-198.6\,[\log_{10}(8.3\times 10^{-4}R_0)+\tfrac{3}{2}\log_{10}T-0.43]-172, \quad (15)$$

which is valid whenever the acoustic scattering relation $\tau_{II,\perp}\propto\epsilon^{\frac{1}{2}}$ is obeyed[4]; the cyclotron masses[36] $m_{II}^*=1.58m$, $m_\perp^*=0.082m$ were assumed. Thus, the temperature difference ΔT between the arms S_1S_2 was obtained by dividing the measured voltage $V_{S_1S_2}$ by the calculated sum Q_e+Q_p. [Departures from the assumptions used in (15) will affect the entries in Table III, but will cancel out in the determination of ΔT.]

Except for a few Nernst measurements at high temperatures with the sample slowly cooling, the measurements were made under steady-state conditions with no temperature drift. The Nernst coefficient,

$$B=1.80V_{NN'}/\Delta TH \text{ volts deg}^{-1}\text{ gauss}^{-1}, \quad (16)$$

TABLE III. Values of Q_p for high-purity n-type germanium determined by subtracting Q_e, Eq. (15), from the measured Q relative to copper (the absolute thermoelectric power of copper is $\lesssim 2$ μv/deg throughout the range shown). The values are believed to be correct to the larger of 30 μv or 3% of Q_p, plus any error in Eq. (15). Below 80°K there is a small dependence on cross-sectional dimension, and below 50°K there are variations from sample to sample, which may get as large as 20% or so at 20°K, due to differences in orientation and variations in the amount of impurity scattering. The values quoted are for the cross-sectional dimensions (Fig. 2) of the samples used and for ∇T in a [100] direction.

T°K	Q_p (μv/deg)	T°K	Q_p (μv/deg)
250	107	80	1040
225	125	70	1450
200	150	60	2040
175	188	50	2940
150	248	40	4300
125	359	30	6400
110	469	20	8700
100	590	15	8600
90	770	10	7000

[35] See, for example, Debye and Conwell, reference 32.
[36] Dresselhaus, Kip, and Kittel, Phys. Rev. **98**, 368 (1955).

was read as a function of about twelve different values of H in the "normal" transverse direction from 100 to 18 000 gauss and repeated in the same fields with H in the "reverse" direction. Then, upon passing an electric current through the sample, the Hall voltage was determined by subtracting the previously measured Nernst voltage in field H from the measured Hall plus Nernst voltage in the same field H. In a similar manner, the transverse ΔQ and $\Delta\rho$ effects were determined by reading voltages $V_{S_1S_2}$ in the same twelve magnetic fields without and with the passage of electric current. The sample was then rotated 90° and the longitudinal ΔQ and $\Delta\rho$ effects measured similarly. Electric currents of the order of 10^{-4} amp were generally used in the saturation (20–250°K) range. A simple, convenient germanium Hall probe,[37] Fig. 4, was used with a 12-in. Varian magnet and regulated power supply to reach the desired fields from 0 to 18 000 gauss quickly and accurately.

Experimental Sources of Error

In this section we shall evaluate the experimental sources of error. Those that are subject to fairly open scrutiny have been minimized to the extent that they do not seriously limit the analysis and interpretation of the data. However, it is possible for more subtle errors to creep into the experiment, and for this reason we have tried to cross check our results.

The known sources of error in the experimental parameters, namely, the average sample temperature, the temperature gradient, and the electric and magnetic fields, are relatively straightforward. The average sample temperature is not required with any great absolute accuracy; however, the estimate from the previously determined resistance-temperature curve (in which a copper-constantan thermocouple was used), or from resistivity calibrations at bath temperature should be good to ±1°. Of course, since the resistivity measurements were made to 0.01%, the relative temperatures in any one series of measurements are known to ~0.01% (except near the conductivity maximum around 20–25°K). The temperature gradient was believed to be known to within ±2% near 77°K, increasing to ±5% below 20°K and at the onset of intrinsic conduction, since this is the spread of the values of Q_e+Q_p for the several samples used to determine Q_p in Table III. As stated previously, any incorrect apportionment of the measured Q between Q_e, Eq. (15), and Q_p will result in errors in the values of Table II, but will automatically compensate in the measurement of the temperature gradient. The magnetic fields were measured to within $(10^{-3}H+1)$ gauss[37]; thus errors due to magnetic field uncertainties are negligible. Voltages were observed to $\sim10^{-6}$ volt (somewhat better for low-field Nernst and ΔQ), noise being the limiting factor. Noise thus placed a lower limit on the magnitude of the magnetic fields that could be used; the smallest Hall angles that could be determined with sufficient precision were of the order of a few degrees. The method of extrapolating to zero field by plotting against H^2 gives added weight to the higher-field results where the errors due to noise become negligible; the details of the extrapolations for obtaining the limiting values for both high and low fields will be described more fully in our forthcoming paper[5] in connection with the quantitative comparison with theory. Errors due to dimensional uncertainties are also negligible since all of the six-armed samples were prepared with the aid of a steel die having tolerances of ±0.003 cm. The actual location of the lead wire on the arm, far away from the body of the sample, varies somewhat, but of course is unimportant. The conclusion of this rather lengthy paragraph is that estimated uncertainties in determining the experimental parameters should cause errors less than ±5% in the final results and that cross comparisons at given resistivities are considerably better.

Considerable cross-checking was done to eliminate other more subtle errors that might otherwise be overlooked. All measurements in the special-purpose apparatus depend on the assumption that the temperature gradient along the axis of the sample, ∇T is independent of magnetic field. This rests on strong theoretical grounds. The heat transport is by lattice conduction for which there should be no magnetothermal effects (the few mobile charge carriers present in the high-purity material can be responsible for only a negligible fraction of the heat transport). Experimentally, within the limits of detection (~0.1% in a field of 5000 gauss) which is much coarser than the anticipated magnitude, this is true. However, there conceivably could be magnetothermal-resistive effects in the copper and solder thermal path between the sample and the bath which would cause the average sample temperature to change during magnetization. This was investigated by comparison of the Hall voltage measured under isothermal conditions when the sample and bath both were at 13.9°K, the triple point of hydrogen, with the Hall voltage measured in a gradient when the average sample temperature was at 13.9°K and the bath was at the boiling point of helium. Any change in sample temperature upon magnetization from 0 to 18 000 gauss was less than 0.04°K. While similar checks could not be made at higher temperatures, where such effects would be expected to be smaller, because the Hall effect is no longer a sensitive function of temperature (saturation range), it was possible to compare the results obtained with different ∇T's and bath temperatures for the same average sample temperature. The most stringent of such tests was made when the average sample temperature was 77°K and the bath was either at the triple point of nitrogen, 63.1°K, or at the boiling point of hydrogen, 20.4°K. The results for B, ΔQ, $\Delta\rho$, and R all agreed to

[37] T. H. Geballe and J. E. Kunzler (to be published).

better than $\frac{1}{2}\%$, a value consistent with the estimated sources of error considered in the preceding paragraph.

In general the sample homogeneity was good; the Hall constant was the same within 1% when measured across arms S_1S_1', N_1N_1', or S_2S_2'. The high-field magnetoresistance did not always saturate as well as expected and the higher purity samples exhibited a small first-order dependence on H which increased at low temperatures. This is assumed to be taken care of by the normal procedure of reversing the magnetic field. Unusual cases will be discussed specifically in our forthcoming paper[5] when necessary. The Nernst voltage occasionally failed to reverse with field in the purer samples at high magnetic fields. In some cases it is believed a small amount of surface conduction can be contributing to the Nernst voltage at the higher temperatures; this will be discussed more fully in Sec. 4.

End effects and side-arm effects can be important sources of error if an unfavorable geometry is used.[38–40] However, the former are negligible for magnetoresistance[39] when the distance from the current leads to the potential arms is $\gtrsim$ twice the width of the specimen, as it is here; their effect on thermomagnetic measurements should be even less. When the magnetic field is parallel to the side-arms their presence can seriously modify the magnetoresistance by shorting the Hall voltage[40]; this effect, which should be much less serious for thermomagnetic effects, was avoided by using only magnetic fields in the horizontal plane of Fig. 5. Even so, some distortion of the electrical and thermal current lines will take place near the side-arms. It is easily shown that when the axes of the specimen are of the [100] type and **H** is normal to the plane of the specimen, all electrical and thermomagnetic quantities are measured with no errors due to side-arms. This has been confirmed experimentally by measurements in a specimen with the middle side-arms removed. For other cases, e.g., for the [100] longitudinal magnetoresistance, a small error is introduced by the current distortions. Half this error disappears when the middle side-arms are removed, and so the total error can be determined. This correction (at most a few %) has been ignored in the graphs below, but is included in the analysis of our forthcoming paper.[5]

4. PRINCIPAL EXPERIMENTAL RESULTS

In this section we shall present, in graphical form, typical samples of the data taken, and shall show that even without use of any more detailed theory than that already presented in Sec. 2, these lead to a number of qualitative and semiquantitative conclusions. We shall discuss the Nernst and the high- and low-field ΔQ results in turn.

[38] R. F. Wick, J. Appl. Phys. **25**, 748 (1956).
[39] J. R. Drabble and R. Wolfe, J. Electronics **3**, 259 (1957).
[40] H. P. R. Frederikse and W. R. Hosler, Phys. Rev. **108**, 1136 (1957).

Nernst Effect

The values of the low-field Nernst coefficient B for the purer specimens seem to agree fairly well with one another; they are plotted against temperature in Figs. 6 and 7. From these plots we note:

(a) *The electron-diffusion B_e predominates at high T, the phonon-drag B_p at low.* The theoretical discussion of Sec. 2 leads us to expect $B_e<0$ and of order $(k/e)(\mu_H/c)$—the actual value for acoustic scattering[41] is -43 μv/deg—and $B_p>0$ and of the order of a sizable fraction of Q_p (μ_H/c). Since Q_p varies rapidly with temperature we should expect B_p to dominate B_e at low T, the reverse at high T. This expectation seems to be confirmed by the fact that B decreases rapidly with increasing T and becomes negative for some specimens above about 175°K. The lack of reproducibility from one specimen to another in the range 175°–250° seems to indicate the presence of a competing conduction mechanism, such as dislocations or surface conduction. The Nernst coefficient is enormously more sensitive to such competition than are the results of purely electrical measurements, and to suppress the expected region of negative B would only

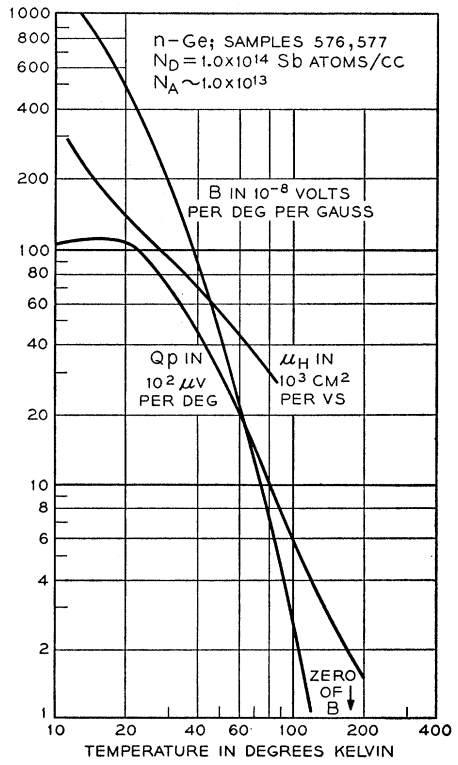

FIG. 6. Typical plot (samples 576 and 577) of the low-field Nernst coefficient B against temperature, in the low-temperature range where B_p is dominant. Also shown are the Hall mobility μ_H and the phonon-drag part of the thermoelectric power $Q_p \equiv Q(\text{meas.}) - Q_e(\text{theor.})$.

[41] See the literature cited in reference 17, or our forthcoming paper.[5]

require that about 2% of the current be carried by the competing mechanisms. Previous observers[42] have failed altogether to find the expected negative B's. The behavior of our specimens 576, 596, 601, and 603 after some sort of aging process, however, encourages the belief that they are normal, and that specimens which do not go negative or go positive again before the onset of intrinsic conduction, such as 594, are imperfect. For one thing, of all our specimens, 601 is the one for which a negative B is most to be expected, since its high carrier concentration would be more likely to swamp out competing mechanisms than would those of the purer specimens, while it is not yet sufficiently highly doped for impurity scattering to drive B_e positive. Secondly, the values observed for this specimen agree fairly well with the theoretically-expected resultant of B_e, B_p, and the effect of intrinsic carriers, as shown by the dashed curve in Fig. 7. Finally, this specimen showed a transverse $\Delta Q/H^2$ ratio which decreased at a reasonable rate with increasing temperature below the intrinsic range. Sample 594, for example, actually showed a slight increase in this ratio, a phenomenon hard to understand on the basis of transport in the conduction band only. All these anomalies deserve further investigation.

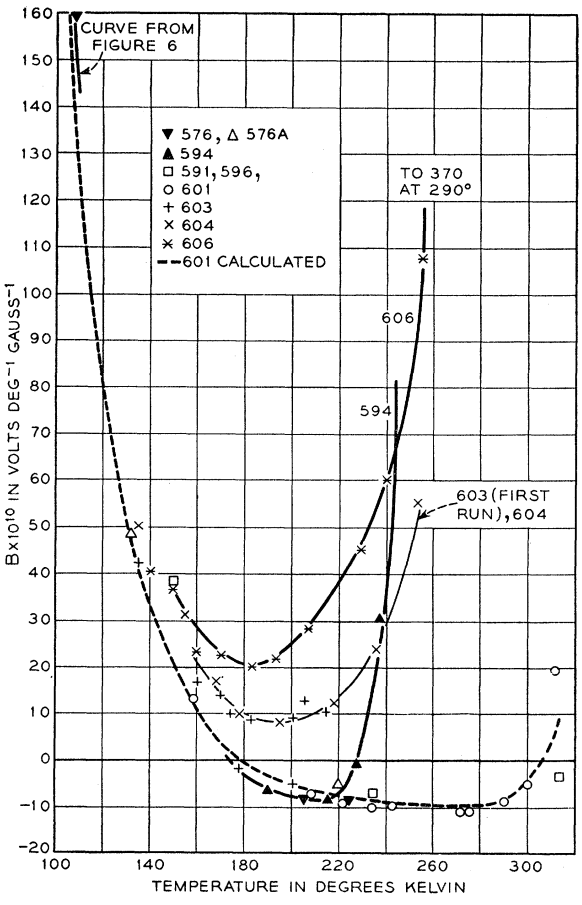

FIG. 7. Plot of the low-field Nernst coefficient B against temperature, for the high-temperature range where B_e becomes dominant. The effect of what are presumed to be changes in surface conduction is manifest in the difference between the two sets of points for sample 603, taken about a month apart. The dashed curve is the behavior which would be expected (including the effects of intrinsic carriers) for sample 601 if B_e had the value for ideal lattice scattering and B_p were given by Eq. (17) with $\zeta_p=0.24$.

[42] Krylova and Mochan, reference 10; Steele, reference 15.

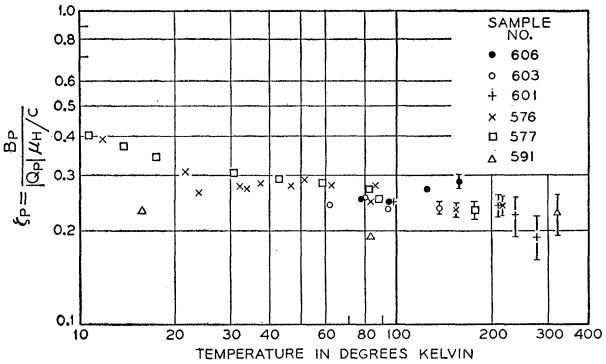

FIG. 8. Values of the dimensionless coefficient ζ_p defined by Eq. (17), as computed using the acoustic-scattering value of B_e. The vertical lines above 100°K represent the uncertainty caused by the estimated uncertainty of ± 15 μv in Q_p. Specimen 591 shows the effect of impurity scattering.

(b) *The ratio of B_p to $Q_p\,\mu_H/c$ is nearly constant.* The interpretation of the low-temperature B as predominantly due to phonon drag receives added confirmation both from the large magnitude of B and from its temperature dependence. Figure 6 shows, along with B, typical values of the Hall mobility μ_H and of the phonon-drag contribution Q_p to the thermoelectric power. Over most of the temperature range the slope of B is roughly equal to the sum of the slopes of μ_H and Q_p, as it should be if the square bracket in the expression (B.4) of Appendix B for B_p is insensitive to T; this in turn is to be expected if the scattering mechanisms vary but little with T. If we define a dimensionless coefficient ζ_p by

$$B_p = B - B_e = \zeta_p |Q_p| \mu_H/c, \qquad (17)$$

and use for B_e the theoretical value[41] $-\frac{1}{2}(k/e)(\mu_H/c)$ for pure acoustic scattering, we find the values of ζ_p shown in Fig. 8. These are in fact nearly constant with temperature near liquid air temperature and above, and the magnitude is of the order of that expected theoretically; a more quantitative interpretation will be given in our forthcoming paper.[5]

(c) *Boundary scattering of the phonons modifies B_p at the lowest temperatures.* Below about 20°K the curve of Q_p in Fig. 6 levels off, because of the transition from phonon-phonon to boundary scattering as the dominant mechanism of equilibration of the phonons. Correspondingly, the curve of B shows a lessening of slope, but continues to rise with decrease of T, because μ_H continues to increase. The values of ζ_p are rather higher in this region that at higher temperatures, a fact which need not be surprising since the altered

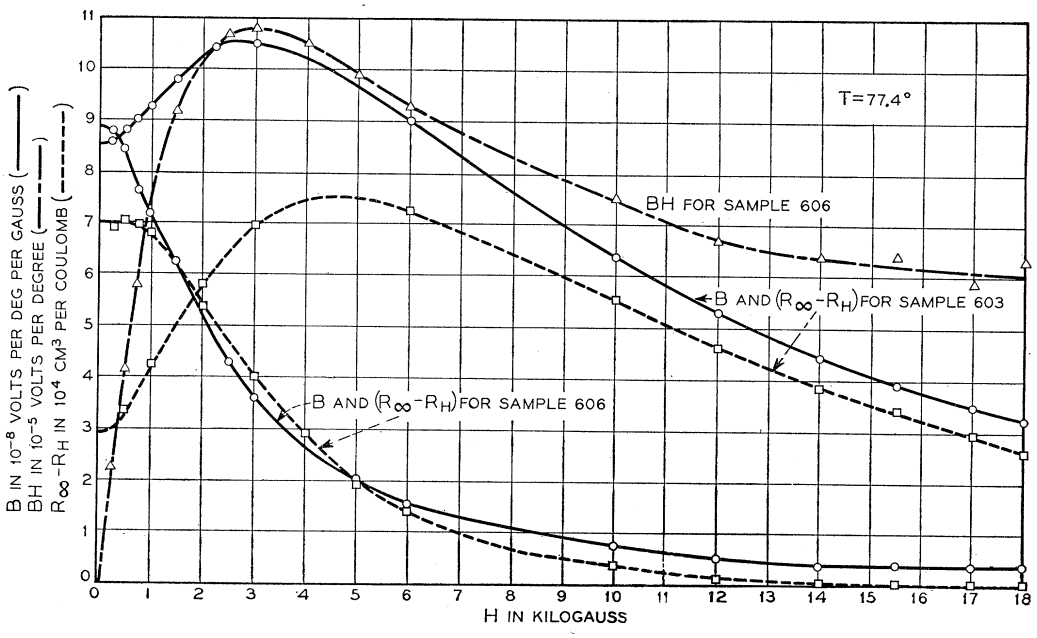

FIG. 9. Comparison of the dependence of the Nernst coefficient B on magnetic field H (full curves) with that of the Hall coefficient R (dashed curves). For sample 606, **H** was along [001], ∇T along [100]; for 603, **H** was along [110], ∇T along [1$\bar{1}$0]. The dot-dash curve shows the behavior of the product BH for 606. All data were taken at 77.4°K.

scattering mechanism for the phonons must alter both the anisotropy and the energy dependence of the partial Peltier coefficients or thermoelectric powers of the different groups of carriers. A more detailed discussion will be given elsewhere.[43]

A typical plot of the variation of Nernst coefficient with magnetic field is shown in Fig. 9 for two orientations. Since the discussion of Sec. 2 leading to (12) suggests that the curve of B_p against H may be qualitatively similar to the inverted curve of Hall coefficient R against H, the latter curve is also shown for the same two specimens. We note:

(d) *As H becomes very large, BH becomes very small.* This agrees with the prediction of Sec. 2.

(e) *The similarity of the curves for B and $R(\infty)-R(H)$ suggests that* $\Pi_{p\parallel} \gg \Pi_{p\perp}$. When **H** is in a [110] direction, the curve of $R(\infty)-R(H)$ at first rises with increasing **H**, then falls off, while when **H** is in a [100] direction the initial rise is much weaker and the ultimate approach to zero is much more rapid. All these features are predicted by theory[44] as consequences of the valley structure and the anisotropy of $\mathbf{m}^*\boldsymbol{\tau}^{-1}$. The curves of $B(\mathbf{H})$ behave in just the same way, except that the initial rise is less pronounced for the [110] case and is absent for the [100] case. This behavior, combined with the fact that the ζ_p's of Fig. 8 are two or more times larger than the value of the square bracket in (12), suggests that the $\mathbf{\Pi}_{pg}$ have an anisotropy similar to that assumed in (12), but less marked. We shall see in a moment that this conclusion is more directly apparent in the anisotropy of ΔQ.

ΔQ at Large Magnetic Fields

Figures 10 and 11 are typical plots of the variation of ΔQ with **H**, for **H**, respectively, parallel and normal to ∇T; for comparison, the corresponding magnetoresistance curves are also shown. At liquid-air temperature the ΔQ curves show a very good approach to saturation for the longitudinal effect and a fair approach for the transverse effect. The saturation of the magnetoresistance curves is slightly poorer. We can draw the following conclusions:

(f) *The high-field ΔQ is dominated by ΔQ_p near liquid-air temperature.* As shown in Sec. 2, as $H \to \infty$, the transverse $-\Delta Q_e$ approaches 43 μv/deg for acoustic scattering. The observed $-\Delta Q$'s in Figs. 10 and 11 range from hundreds to thousands of μv/deg, the largest effect being when **H** and ∇T are both in the same [100] direction.

(g) *The anisotropy of ΔQ shows that* $\Pi_{p\parallel}/\Pi_{p\perp}$ *is* $\gg 1$ *but* $<m_\parallel{}^*\tau_\perp/m_\perp{}^*\tau_\parallel$. The large magnitude of ΔQ_p and its great anisotropy must arise from an anisotropy of the partial Peltier coefficients $\mathbf{\Pi}_{pg}$ of the energy shells in different valleys. For if the $\mathbf{\Pi}_{pg}$ were isotropic the change of Q_p, or equivalently of $\mathbf{j}\cdot\sum \mathbf{\Pi}_{pg}\cdot\mathbf{j}_g/j^2$, with H, would have to be entirely due to the change of the distribution of current among groups of different energy ϵ, combined with whatever variation of $\mathbf{\Pi}_{pg}$ with ϵ might be present. This would give no anisotropy of the transverse ΔQ_p at infinite field, and unless $\mathbf{\Pi}_{pg}$ increased

[43] T. H. Geballe and C. Herring (to be published).
[44] W. M. Bullis and W. E. Krag, Phys. Rev. **101**, 580 (1956).

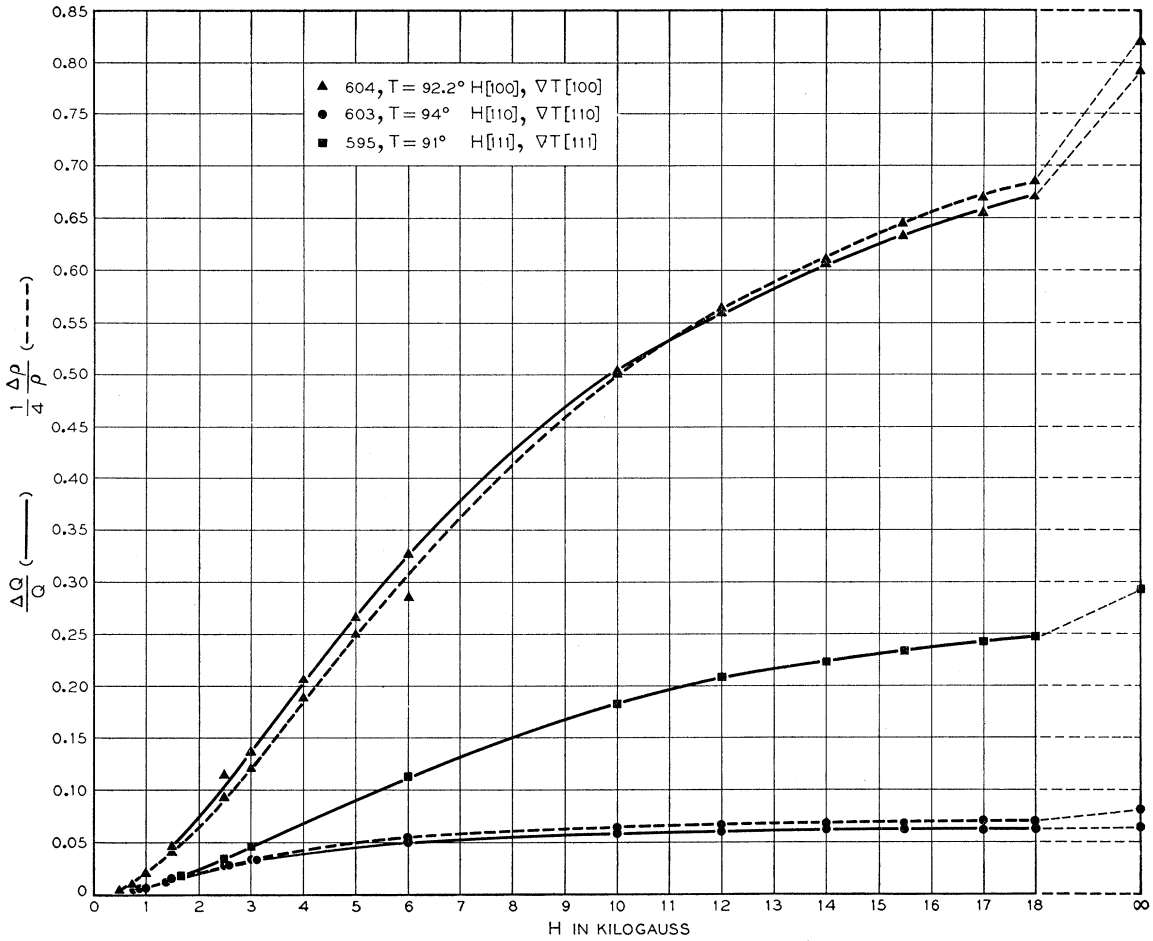

FIG. 10. Typical curves of longitudinal ΔQ and longitudinal magnetoresistance, for three orientations. The values indicated for infinite magnetic field are obtained by a parabolic extrapolation of the high-field data against H^{-2}.

enormously with increasing energy, it could not give as large an effect as is observed. If, on the other hand, $\Pi_{p||}/\Pi_{p\perp}$ were equal to $m_{||}{}^*\tau_\perp/m_\perp{}^*\tau_{||}$, and $\Pi_{p||}$, $\Pi_{p\perp}$ were both proportional to $\epsilon^{\frac{1}{2}}$, the theorem of Sec. 2 says that $\Delta Q_p/Q_p$ would equal $\Delta\rho/\rho$ in every orientation and magnetic field. For the longitudinal cases at infinite field, this equality is unchanged by any alteration in the energy dependence of $\Pi_{p||}$ and $\Pi_{p\perp}$, as long as their ratio has the value just specified; this is because the distribution of the $\mathbf{j}_q$'s in energy is the same at $H=0$ and ∞ when $\mathbf{E}$ and $\mathbf{H}$ are parallel.[20] For the conditions of Fig. 10, $Q/Q_p\approx 3$, so $\Delta Q_p/Q_p\approx\frac{3}{4}\Delta\rho/\rho$; thus we conclude that $\Pi_{p||}/\Pi_{p\perp}$ is much greater than 1 but appreciably less than $m_{||}{}^*\tau_\perp/m_\perp{}^*\tau_{||}$, which latter quantity is about 17 for the specimens shown. For the transverse cases, a comparison of Fig. 11 with Fig. 10 shows that $\Delta Q/\Delta\rho$ is smaller than for the longitudinal; this can be correlated[5] with the fact to be brought out in item (i) below, that the energy dependence of $\Pi_{p||}$ and $\Pi_{p\perp}$ differs from that assumed in the theorem of Sec. 2.

ΔQ at Small Magnetic Fields

Figure 12 shows the low-field limit of $(c/\mu_H H)^2\Delta Q$ for two orientations at various temperatures. In the electron-group approximation the values for these two orientations should determine the values for all other orientations, since according to (4) all low-field ΔQ's are expressible in terms of the three constants q_b, q_c, q_d and since for electron-group conduction in [111] valleys it can be shown (Appendix C) that $q_b=-q_c$, a relation analogous to the more familiar one[6,19,20] for the magnetoresistance constants b, c, d. Figure 13 shows, for the single temperature 94°K, how well the values of $(c/\mu_H H)^2\Delta Q$ and of $(c/\mu_H H)^2(\Delta\rho/\rho)$ measured on different samples obey the expected symmetry relations. The departures from the latter, which are nearly the same at all the temperatures studied, are fairly small, and are of similar magnitude for both ΔQ and $\Delta\rho$. The data might have been fitted a trifle better with $q_b+q_c<0$, $b+c<0$. But as the latter unequality, according to Appendix C, is impossible in pure material, we prefer to regard the discrepancies as due to de-

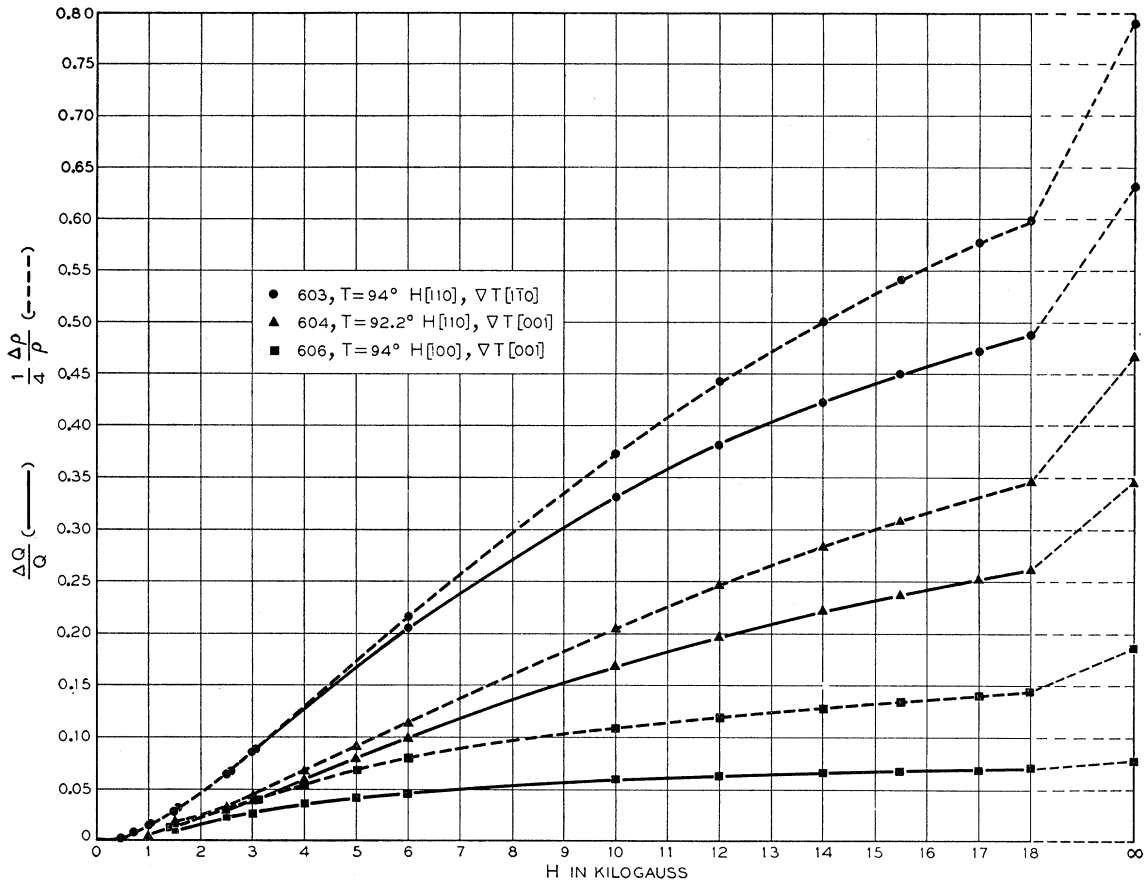

FIG. 11. Typical curves of transverse ΔQ and transverse magnetoresistance, for three orientations. The values indicated for infinite magnetic field are obtained by a parabolic extrapolation of the high-field data against H^{-2}.

partures from ideal experimental conditions, rather than from $q_b+q_c=b+c=0$.

The data of Fig. 12 confirm, at least roughly, the general conclusions we have already drawn from the Nernst and high-field data, and we shall show that they lead to an additional conclusion in regard to the energy variation of the partial Peltier coefficient of an energy shell. Specifically, we note:

(h) *Conclusions* (f) *and* (g) *above are reaffirmed.* The magnitude and temperature variation of $\Delta Q/H^2$ indicate a large contribution from ΔQ_p near liquid-air temperature. Whereas $(c/\mu_H H)^2\Delta Q_e$ should be independent of T, at least in the lattice-scattering range, the observed values of $(c/\mu_H H)^2\Delta Q$ increase more and more rapidly with decreasing T, eventually about as fast as Q_p. The anisotropy of $\Delta Q/H^2$ again resembles that of the magnetoresistance (longitudinal [100] effect the highest, etc.) but is somewhat less marked. As before, this suggests that $\Pi_{p||}/\Pi_{p\perp}\gg 1$ but $<m_{||}{}^*\tau_\perp/m_\perp{}^*\tau_{||}$.

(i) *The significant average of* $\Pi_{p||}$ *and* $\Pi_{p\perp}$ *decreases slightly with increasing electron energy.* This conclusion can be drawn, assuming nothing more than the electron-group picture, from the data for $H\|[001]$, $\nabla T\|[100]$. Although we shall put the analysis into quantitative form in our forthcoming paper,[5] it will be worthwhile to show here how the conclusion can be obtained qualitatively with a minimum of equations and assumptions.

Consider the empirically measurable

$$\Delta\bar{Q}\equiv\Delta Q_{100}{}^{001}-B_{100}{}^{001}HR_{100}{}^{001}H(\rho_{100}{}^{001})^{-1}$$
$$=\Delta Q_{100}{}^{001}+BH(\mu_H H/c) \quad \text{for low fields, } n\text{-type material.} \quad (18)$$

Some values of this $\Delta\bar{Q}$ divided by the square of the Hall angle are plotted in Fig. 14. It is easily shown (Appendix D) that $\Delta\bar{Q}$ represents the change in the thermoelectric emf $\bar{Q}$ per unit temperature difference between two infinite plane-parallel electrodes normal to the [100] direction, i.e., in the thermoelectric power measured under the condition ∇T and $\mathbf{E}\|[100]$, $j_x=0$, j_y unconstrained. We shall show that $\Delta\bar{Q}$ depends on the variation of the $\mathbf{\Pi}_g$'s of the different shells with energy, but not, for given Q_p, on their anistropy.

The first step in the argument is to show that if by analogy to (13) we define $\bar{Q}_g$ to be the partial thermoelectric power which any energy-shell group g of

electrons would possess under the conditions just stated (∇T and $E\|[100]$, $j_{gx}=0$), then

$$\bar{Q}_g(\mathbf{H})+\bar{Q}_g(-\mathbf{H}) \tag{19}$$

is independent of $\mathbf{H}$ when $\mathbf{H}$ is normal to ∇T. The proof of this, although almost nonmathematical, involves details which might distract the reader, and we have therefore relegated it to Appendix D. The second step is to note that for [111] valleys and the orientation assumed, the quantity (19) is the same for shells of a given energy in each of the four valleys. The third step is to note that for four such shells in parallel, each of energy ϵ to $\epsilon+d\epsilon$, the total thermoelectric power $\bar{Q}_\epsilon(\mathbf{H})$ is even in $\mathbf{H}$, hence equal to half of the common value of (19), which we have just seen to be independent of H. The final conclusion follows from the fact that

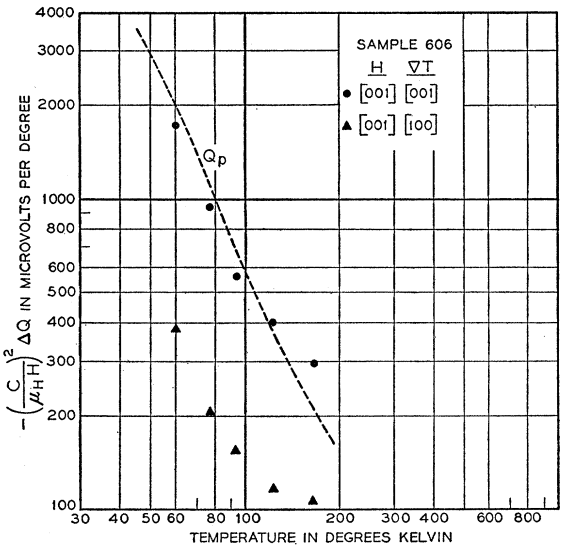

FIG. 12. Temperature variation of the low-field $(c/\mu_H H)^2\Delta Q$ for $\mathbf{H}$ and ∇T both $\|$ [001] and for $\mathbf{H}\|[001]$, $\nabla T\|[100]$. For comparison, the dashed curve shows the variation of Q_p. If the wave-number dependence of the electronic and phonon scattering laws is the same at all temperatures, $(c/\mu_H H)^2\Delta Q_e$ should be constant and $(c/\mu_H H)^2\Delta Q_p$ should be proportional to Q_p.

the $\bar{Q}$ of the entire medium is an average of the $\bar{Q}_\epsilon$ with weights proportional to the contributions of the different energy ranges to the conductivity in the x direction. Namely, this average $\bar{Q}$ will be independent of H if $\bar{Q}_\epsilon$ is independent of energy, and it will be unaffected by changes in the anisotropy of the Q_g which do not alter the $\bar{Q}_\epsilon$. These statements hold for any H, large or small.

Since for lattice scattering the application of a magnetic field reduces the fraction of the current which is carried by the low-energy electrons, we expect the sign of the phonon-drag part of (18) to be the same as (opposite to) that of Q_p if $|\Pi_{p\|}|$ and $|\Pi_{p\perp}|$ increase (decrease) with increasing electron energy. Figure 14 shows how the $\Delta\bar{Q}$ of (18) varies with temperature. At high temperatures $\Delta\bar{Q}$ has the same sign as Q (negative),

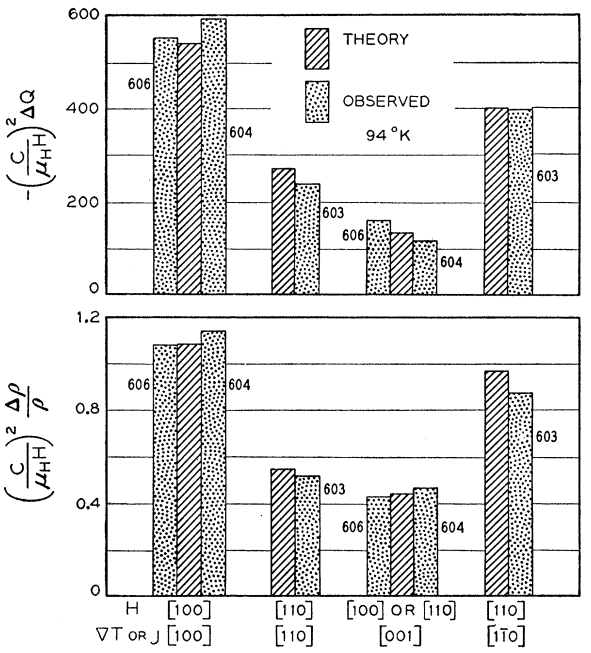

FIG. 13. Typical comparison of low-field ΔQ and magnetoresistance data with predictions based on crystal symmetry. In the top diagram the diagonally-striped bars represent the predictions of Eq. (4) with the ratios of q_b $(=-q_c)$ and q_d to $(\mu_H/c)^2$ chosen equal to 130 and 540 μv/deg, respectively; the speckled bars represent observed values of $-(c/\mu_H H)^2\Delta Q$ at 94°K measured on three specimens in various orientations. In the lower diagram is the corresponding comparison for magnetoresistance at this temperature, $\Delta Q_{\alpha\alpha}$ in (4) being replaced by $\Delta\rho/\rho$ and q_b, q_c, q_d by b, c, d, respectively. The striped bars are drawn assuming the ratios of b $(=-c)$ and d to $(\mu_H/c)^2$ to be 0.43 and 1.08, respectively.

as one would expect if the electron-diffusion contribution predominates. Near liquid-air temperature it is starting to go positive, and this shows not only that the phonon-drag contribution is becoming dominant, but that the appropriate average of $|\Pi_{p\|}|$ and $|\Pi_{p\perp}|$ decreases with increasing electron energy. This is the direction of variation which is to be expected if the relaxation times $\tau_{\rm ph}(q)$ of the phonons increase sufficiently rapidly with decreasing wave number. However, $\Delta\bar{Q}$ is only starting to go positive in a temperature range where the phonon-drag part of most of the thermo-

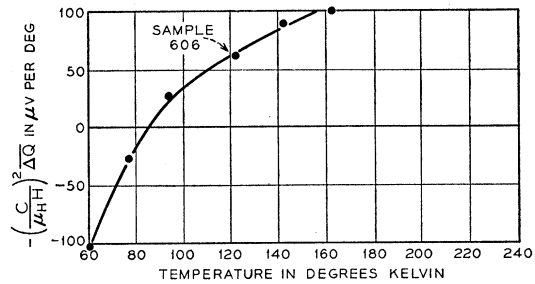

FIG. 14. Temperature variation of the low-field $\Delta\bar{Q}$, Eq. (18), i.e., of the change in thermoelectric power which would be observed with plane-parallel electrodes normal to [100], for $\mathbf{H}\|[001]$.

magnetic quantities is greatly predominant over the electronic part. One can conclude that the dependence of $\Pi_{p||}$ and $\Pi_{p\perp}$ on energy is rather slight, i.e., slower than the first-power dependence of Π_{eg} in something like the ratio of k/e to Q_p at the temperature where $\Delta\bar{Q}$ goes through zero. This ratio is of the order of 0.1. Our present qualitative conclusion is confirmed and refined by the detailed analysis of the following paper.

Significance of the Results

Beyond the general confirmation of the theory and the verification of the expected importance of phonon-drag effects, our principal conclusions are that $\Pi_{p||}/\Pi_{p\perp}$ is of the order of, but less than, the ratio $m_{||}{}^*\tau_\perp/m_\perp{}^*\tau_{||}$, which is known to be about 17 near liquid-air temperature,[5,31] and that the significant average of $\Pi_{p||}$ and $\Pi_{p\perp}$ decreases slowly with increasing energy. Let us consider the latter conclusion first.

The interest of the energy variation of $\Pi_{p||}$ and $\Pi_{p\perp}$ is of course in what it tells us about the phonon-phonon scattering. It is not hard to show that if the relaxation time $\tau_{\rm ph}(\mathbf{q})$ of a mode of wave number $\mathbf{q}$ were of the form $q^n\times$(function of direction), then for ideal lattice scattering we would have $\Pi_{p||,\perp}\propto\epsilon^{\frac{1}{2}+\frac{1}{2}n}$. For the heat flux in the low-frequency phonon system is proportional to the crystal momentum in this system,[3,4] hence to the product of an average $\tau_{\rm ph}$ with the rate of loss of crystal momentum by the electrons to the phonons. The contribution to the heat flux from an energy-shell group g of energy ϵ is thus, for any given orientation,

$$\mathbf{\Pi}_{pg}\cdot\mathbf{j}_g\propto\left[\boldsymbol{\tau}(\epsilon)\right]^{-1}\cdot\mathbf{m}^*\cdot\mathbf{j}_g\tau_{\rm ph}(\bar{q})\propto\epsilon^{\frac{1}{2}+\frac{1}{2}n}j_g, \qquad (20)$$

since the effective phonon wave number $\bar{q}\propto\epsilon^{\frac{1}{2}}$, while $\tau(\epsilon)\propto\epsilon^{-\frac{1}{2}}$.

Now it has been shown[7] that if three-phonon collisions are the dominant source of relaxation, then in the limit $q\rightarrow 0$

$$\begin{aligned}\tau_{\rm ph}(\mathbf{q})&\propto q^{-2}\text{ for longitudinal modes}\\&\propto q^{-1}\text{ for transverse modes}\end{aligned} \qquad (21)$$

provided the dispersion of the longitudinal modes is normal, i.e., highest group velocity at long wavelengths. If the q's of the modes which scatter the electrons are small enough to make (21) a good approximation but not so small that four-phonon, relaxation, or other effects dominate the scattering, then $\mathbf{\Pi}_{pg}$ should be dominated by longitudinal modes, and should go as $\epsilon^{-\frac{1}{2}}$. The observed behavior is not consistent with as rapid a variation as this, and indicates either that the relaxation times of the transverse modes are at least as long as those of the longitudinal ones, or that for some reason the longitudinal modes do not approximate the "ideal" behavior (21) very well. The same conclusion has been reached from an analysis of the temperature variation of Q_p combined with the temperature variation of the effects of specimen diameter on Q_p and on the thermal conductivity[3,8]; the present analysis is cleaner in that it is based on data taken at a single temperature. In our forthcoming paper[5] we shall separate out the energy variations of $\Pi_{p||}$ and $\Pi_{p\perp}$, and in later publications we shall correlate these with the deformation-potential theory of electron-phonon interaction.

Now let us consider the anisotropy of $\mathbf{\Pi}_{pg}$. When we introduced $\mathbf{\Pi}_{pg}$ in Sec. 2, we showed that if $\tau_{\rm ph}$ were the same for all modes, $\Pi_{p||}/\Pi_{p\perp}$ would equal $m_{||}{}^*\tau_\perp/m_\perp{}^*\tau_{||}$. According to deformation-potential theory[6] for n-type germanium $\tau_{||}$ is principally determined by longitudinal modes of large q, $\tau_\perp$ by transverse modes of small q. Thus the fact that the anisotropy of $\mathbf{\Pi}_{pg}$ is less than that of $\boldsymbol{\tau}^{-1}\cdot\mathbf{m}^*$ may be due in part to the increase of $\tau_{\rm ph}$ with decreasing q, in part to the difference between the $\tau_{\rm ph}$'s of the longitudinal and transverse branches, and in part to anisotropy of the $\tau_{\rm ph}$'s within any one branch. In the sequel[5] and later papers we shall try to disentangle these factors.

ACKNOWLEDGMENTS

We are indebted to G. W. Hull and P. Liberti for preparation of the samples and for assistance with the measurements and to E. Buehler and L. P. Adda for supplying the crystals. The presentation has benefited from helpful comments by A. R. Hutson and P. A. Wolff.

APPENDIX A. CONSEQUENCES OF CRYSTAL SYMMETRY

Let $\mathbf{H}$ be along a 2-, 3-, or 4-fold symmetry axis. If this axis is chosen as the x direction, then the axial symmetry alone requires the thermoelectric-power tensor to have the form

$$\begin{bmatrix}Q_{11}&Q_{12}&0\\-Q_{12}&Q_{11}&0\\0&0&Q_{33}\end{bmatrix}\quad\text{(3- or 4-fold axis)}, \qquad (A.1)$$

$$\begin{bmatrix}Q_{11}&Q_{12}&0\\Q_{21}&Q_{22}&0\\0&0&Q_{33}\end{bmatrix}\quad\text{(2-fold axis)}. \qquad (A.2)$$

If now there is present a reflection plane through the symmetry axis, then Q_{11}, Q_{22}, and Q_{33} must be even functions of $\mathbf{H}$, Q_{12} and Q_{21} odd functions, provided that, in the twofold case, the x or y direction is taken normal to the reflection plane. All the experiments reported in the present pair of papers have $\mathbf{H}$ in such symmetry directions, so (A.1) and (A.2) will always apply. It is worth noting that, in the expression (A.2), Q_{12} is in general different from $-Q_{21}$, though to the first order in $\mathbf{H}$ it is not.[45] This behavior differs from that of the conductivity tensor, for which the Onsager relations require the part odd in $\mathbf{H}$ to be antisymmetric. It leads to the interesting prediction that when $\mathbf{H}$ and

[45] This lack of symmetry has been noticed before: J. Meixner, Ann. Physik **40**, 165 (1941); M. Kohler, Ann. Physik **40**, 601 (1941).

∇T are not in symmetry directions the thermoelectric power measured along ∇T should be slightly different for $\mathbf{H}$ and $-\mathbf{H}$.[46]

The relations just derived, combined with (1) and (2), show that if $\mathbf{H}$ is along a 3- or 4-fold symmetry axis, or for any direction of ∇T in a cubic crystal if $\mathbf{H}$ is infinitesimal,

$$Q_{\beta\alpha}=B\sum_\gamma H_\gamma\delta_{\gamma\alpha\beta}, \tag{A.3}$$

where the α direction is along ∇T and $\delta_{\gamma\beta\alpha}=\pm1$ if $\gamma\beta\alpha$ is an even (odd) permutation of 123, zero otherwise. Except in the limit $H\rightarrow 0$, B depends on the magnitude and direction of $\mathbf{H}$; B is an even function of $\mathbf{H}$, whenever $\mathbf{H}$ is along a 3- or 4-fold axis, or if $\nabla T\perp\mathbf{H}$ is in a symmetry direction when $\mathbf{H}$ is along a 2-fold axis. These cases cover all the arrangements used in the present experiments. For more general orientations one must (just as for the Hall coefficient) either modify the definition (3) or allow B to contain odd powers of $\mathbf{H}$.

APPENDIX B. THE LOW-FIELD NERNST COEFFICIENT

The low-field Nernst coefficient is related, by (3) and (5), to the part of $\mathbf{\Pi}$ that is antisymmetric and of the first order in H. By (8) the first-order part of $\mathbf{\Pi}$ is

$$\begin{aligned}\mathbf{\Pi}^{(1)}&=\sum_g\mathbf{\Pi}_g\cdot(\boldsymbol{\sigma}_g^{(1)}\cdot\boldsymbol{\varrho}^{(0)}+\boldsymbol{\sigma}_g^{(0)}\cdot\boldsymbol{\varrho}^{(1)})\\&=\sum_g(\mathbf{\Pi}_g-\mathbf{\Pi}^{(0)})\cdot(\boldsymbol{\sigma}_g^{(1)}\cdot\boldsymbol{\varrho}^{(0)}+\boldsymbol{\sigma}_g^{(0)}\cdot\boldsymbol{\varrho}^{(1)}),\end{aligned} \tag{B.1}$$

since the sum on g of the second factor is zero by the definition of $\boldsymbol{\varrho}$ (any constant could have been used in place of $\mathbf{\Pi}^{(0)}$). Now for cubic material

$$\rho_{\alpha\beta}^{(1)}=-R\sum_\gamma\delta_{\alpha\beta\gamma}H_\gamma, \tag{B.2}$$

where R is the Hall constant. For extrinsic material we can set $R/\rho^{(0)}=\mp\mu_H/c$, where μ_H is the Hall mobility and the upper sign is for n type, the lower for p. If we choose the z direction along H and define the tensor $\mathbf{\Omega}$ by $\Omega_{xy}=-\Omega_{yx}=1$, other components$=0$, we have

$$B=\frac{\Pi_{xy}^{(1)}}{H}=\Pi^{(0)}\left[\sum_g\left(\frac{\mathbf{\Pi}_g}{\Pi^{(0)}}-1\right)\cdot\left(\frac{\boldsymbol{\sigma}_g^{(1)}}{H\sigma^{(0)}}\pm\frac{\boldsymbol{\sigma}_g^{(0)}\cdot\mathbf{\Omega}}{\sigma^{(0)}}\frac{\mu H}{c}\right)\right]_{xy}. \tag{B.3}$$

Since $\Pi^{(0)}=\mp|Q^{(0)}|T$ we have finally, for extrinsic material,

$$B=|Q^{(0)}|\frac{\mu H}{c}\left[\sum_g\left(\frac{\mathbf{\Pi}_g}{\Pi^{(0)}}-1\right)\cdot\left(\frac{\boldsymbol{\sigma}_g^{(1)}}{\mp(\mu_H H/c)\sigma^{(0)}}-\frac{\boldsymbol{\sigma}_g^{(0)}\cdot\mathbf{\Omega}}{\sigma^{(0)}}\right)\right]_{xy}. \tag{B.4}$$

This equation is essentially the same as Eq. (46) of reference 3. It has the form of a correlation between fluctuations of the $\mathbf{\Pi}_g$ about $\Pi^{(0)}\mathbf{1}$ and fluctuations of the $\boldsymbol{\sigma}_g^{(1)}$ about the reference values $\mp(\mu_H H/c)\boldsymbol{\sigma}_g^{(0)}\cdot\mathbf{\Omega}$. The expression applies to B_e or B_p as well as to the total B, if $Q^{(0)}$, $\mathbf{\Pi}_g$, $\Pi^{(0)}$ are given the appropriate subscript. Note that the vanishing of the sum of the second factor in (B.4) is the definition of μ_H, and the vanishing of the sum of the first factor times $\sigma_g^{(0)}$ is the definition of $\Pi^{(0)}$. Therefore either the $-\mathbf{1}$ in the first factor of the sum or the $\boldsymbol{\sigma}_g^{(0)}\cdot\mathbf{\Omega}/\sigma^{(0)}$ in the second factor (but not both) may be omitted without changing the value of (B.4).

APPENDIX C. SYMMETRY RELATIONS AMONG q_b, q_c, q_d, OR AMONG THE MAGNETORESISTANCE CONSTANTS

We have introduced, in (4), three constants q_b, q_c, q_d which describe the low-field ΔQ in a cubic crystal. The familiar magnetoresistance constants[22] b, c, and d are defined by an equation of identical form for $\Delta\rho_{\alpha\alpha}/\rho$. It is well known[6,19,20] that b, c, and d satisfy a symmetry relation derivable from the valley structure. Here we shall show that, to the accuracy of the electron-group approximation using energy shells, the q's have a like symmetry,

$$b+c=0,\quad q_b+q_c=0\quad\text{for [111] valleys,} \tag{C.1}$$

$$b+c+d=0,\quad q_b+q_c+q_d=0\quad\text{for [100] valleys,} \tag{C.2}$$

and that regardless of the validity of this approximation

$$b+c\geq 0\quad\text{for [111] valleys,} \tag{C.3}$$

$$b+c+d\geq 0\quad\text{for [100] valleys,} \tag{C.4}$$

for sufficiently pure material. The relation (C.4) is well known, as it expresses the non-negativity of the longitudinal [100] magnetoresistance; (C.3) does not seem to have been pointed out before. No such general inequalities hold for the q's.

The assumption basic to all parts of our argument is that in isothermal conduction the current and heat flux are each a sum of contributions from carriers in the different valleys, the relation of each such contribution to the electric and magnetic field strengths being governed by the symmetry of the valley. This can fail only if the scattering of carriers in one valley is affected by the current in another valley, e.g., in the presence of electron-electron scattering[47] or saturation[3] of the phonon-drag effect. At low carrier densities the assumption must always be valid.

It will be convenient to express q_b, q_c, and q_d in terms of components of a fourth-rank tensor. If we write (4) in the form

$$Q_{\alpha\beta}^{(2)}=\sum_{\gamma\delta}q_{\alpha\beta\gamma\delta}H_\gamma H_\delta, \tag{C.5}$$

[46] This difference seems actually to have been observed: E. Grüneisen and J. Gielessen, Ann. Physik **27**, 243 (1936) (Bi); E. Grüneisen and H. D. Erfling, Ann. Physik **36**, 357 (1939) (Be).

[47] R. W. Keyes, J. Phys. Chem. Solids (to be published).

then for $\alpha \neq \beta$ along cube-edge directions,

$$q_b = q_{\alpha\alpha\beta\beta}, \tag{C.6}$$

$$q_c = 2q_{\alpha\beta\alpha\beta}, \tag{C.7}$$

$$q_b + q_c + q_d = q_{\alpha\alpha\alpha\alpha}. \tag{C.8}$$

Note that $q_{\alpha\beta\gamma\delta}$ is symmetrical in the first two and in the last two suffixes, even though for a general finite H the tensor $Q_{\alpha\beta}(\mathbf{H}) + Q_{\alpha\beta}(-\mathbf{H})$ need not be symmetrical.

Let us write for the contribution of valley i to the heat flux

$$\mathbf{F}_i(\mathbf{H}) = \mathbf{G}_i(\mathbf{H}) \cdot \mathbf{E}, \tag{C.9}$$

so that

$$\mathbf{\Pi}(\mathbf{H}) = \sum_i \mathbf{G}_i(\mathbf{H}) \cdot \boldsymbol{\varrho}. \tag{C.10}$$

The part of this which is of the second order in H is

$$\mathbf{\Pi}^{(2)} = (\sum_i \mathbf{G}_i^{(2)}) \cdot \boldsymbol{\varrho}^{(0)} + (\sum_i \mathbf{G}_i^{(1)}) \cdot \boldsymbol{\varrho}^{(1)} + (\sum_i \mathbf{G}_i^{(0)}) \cdot \boldsymbol{\varrho}^{(2)}. \tag{C.11}$$

Here $\boldsymbol{\varrho}^{(2)}$ can be expressed in terms of the zeroth-, first-, and second-order parts of the conductivity tensor $\boldsymbol{\sigma} = \sum_i \boldsymbol{\sigma}_i$:

$$\boldsymbol{\varrho}^{(2)} = -[\boldsymbol{\sigma}^{(2)}/(\sigma^{(0)})^2] + [\boldsymbol{\sigma}^{(1)} \cdot \boldsymbol{\sigma}^{(1)}/(\sigma^{(0)})^3]. \tag{C.12}$$

The expression which results when (C.12) is inserted into (C.11) contains two terms with superscript 1's; the $\alpha\beta$ component of either of these contains

$$\sum_\mu \delta_{\alpha\mu\lambda} H_\lambda \delta_{\mu\beta\gamma} H_\gamma = H_\alpha H_\beta - H^2 \delta_{\alpha\beta}, \tag{C.13}$$

and it is easy to show that these terms satisfy (C.1) and (C.2). The remaining two terms in $\mathbf{\Pi}^{(2)}$ each have the form of a multiple of the unit tensor times a sum of $\mathbf{G}_i^{(2)}$ or $\boldsymbol{\sigma}_i^{(2)}$. So we need now only prove that such sums satisfy (C.1) or (C.2). In doing this we need consider only the symmetrical part of $\mathbf{G}_i^{(2)}$, since all the other terms in (C.11) are symmetrical.

We are thus led to consider the properties of the fourth-rank tensor $\bar{G}_{\alpha\beta\gamma\delta}$ whose inner product with $H_\gamma H_\delta$ gives the symmetrical part of the $\mathbf{G}_i^{(2)}$ of a valley. For a valley whose symmetry group contains a three- or four-fold axis and reflection planes through the axis, the symmetry of $\bar{G}_{\alpha\beta\gamma\delta}$ in each pair of suffixes and the symmetry of the coordinate directions 1 and 2 suffice to reduce the number of independent components to seven. If direction 3 is along the symmetry axis, these are the components (1111), (3333), (1122), (1133), (3311), (1212), and (1313). The symmetry with regard to axial rotations gives the further relation

$$\bar{G}_{1111} = \bar{G}_{2211} + 2\bar{G}_{1212}. \tag{C.14}$$

For six [100] valleys the validity of (C.2) depends, according to (C.8), on the vanishing of

$$\tfrac{1}{2} \frac{\partial^2}{\partial H_\alpha^2} [\sum_i \mathbf{G}_i^{(2)}]_{\alpha\alpha} = 2[\bar{G}_{3333} + 2\bar{G}_{1111}]. \tag{C.15}$$

For four [111] valleys (C.6) and (C.7) show that to prove (C.1) we must prove the vanishing of

$$\tfrac{1}{2} \frac{\partial^2}{\partial H_\beta^2} [\sum_i \mathbf{G}_i^{(2)}]_{\alpha\alpha} + \frac{\partial^2}{\partial H_\alpha \partial H_\beta} [\sum_i \mathbf{G}_i^{(2)}]_{\alpha\beta},$$

a quantity for which a short calculation, using (C.14), gives the expression

$$\tfrac{4}{3}[\bar{G}_{3333} + 2\bar{G}_{1111}]. \tag{C.16}$$

Now in the electron-group approximation the longitudinal magnetoconductivity of any energy-shell group vanishes along each of its principal axes, so (C.15) or (C.16) will vanish when $\boldsymbol{\sigma}_i^{(2)}$ is substituted for $\mathbf{G}_i^{(2)}$. These expressions vanish equally well for the $\mathbf{G}_i^{(2)}$ themselves, since the contribution of any energy shell g to $\mathbf{G}_i^{(2)}$ is just $\mathbf{\Pi}_g \cdot \boldsymbol{\sigma}_g^{(2)}$, and $\mathbf{\Pi}_g$ is diagonal in our coordinate system. Therefore (C.1) or (C.2) holds in this approximation. If the electron-group approximation is abandoned, the expression obtained from (C.15) or (C.16) by substituting $\boldsymbol{\sigma}$'s for $\mathbf{G}$'s is always ≤ 0, since the longitudinal magnetoconductivity of a valley is always ≤ 0. This establishes (C.3) or (C.4).

APPENDIX D. PROPERTIES OF THE $\bar{Q}$ OF (18)

For an open circuit between plane-parallel electrodes normal to the x direction we have, if ∇T is in this direction and $\mathbf{H}$ is in the z direction,

$$0 = j_x = \sigma_{xx}[E_x - Q_{xx}(dT/dx)] - \sigma_{xy} Q_{yx} (dT/dx), \tag{D.1}$$

$$\bar{Q}(dT/dx) \equiv E_x = [Q_{xx} + (\sigma_{xy}/\sigma_{xx}) Q_{yx}](dT/dx). \tag{D.2}$$

We are interested in the case where the x, y, and z directions are cube-edge directions; for this case, $\sigma_{xy}/\sigma_{xx} = -\rho_{xy}/\rho_{xx}$ and so

$$\bar{Q} = Q_{100}^{001} - (R_{100}^{001} B_{100}^{001} H^2/\rho_{100}^{001}), \tag{D.3}$$

in agreement with (18).

For any energy-shell group g, let $\bar{Q}_g$ be defined as the ratio of E_x to dT/dx which makes $j_{gx} = 0$ for $E_y = E_z = 0$. Our first task is to prove that when $\mathbf{H}$ is in the z direction, i.e., normal to ∇T,

$$\bar{Q}_g(\mathbf{H}) + \bar{Q}_g(-\mathbf{H}) = 2\bar{Q}_g(0). \tag{D.4}$$

We shall first prove this to the second order in H, and then sketch briefly how it can be proved for arbitrary $\mathbf{H}$. Suppose $\mathbf{E}$ to be such that the electron group in question gives $j_{gx} = 0$ at $H = 0$, j_{gy} and j_{gz} being in general $\neq 0$. Application of a magnetic field will subject this group to a Lorentz force arising from j_{gy}. This will give a first-order contribution $\delta_1 \mathbf{j}_g$ to the current of the group, with, in general, components in all three coordinate directions. The currents $\delta_1 j_{gx}$ and $\delta_1 j_{gy}$ will in turn have Lorentz forces exerted on them, which will produce a second-order current $\delta_2 \mathbf{j}_g$. But it is easily verified that the contributions to $\delta_2 j_{gx}$ arising from $\delta_1 j_{gx}$ and from $\delta_1 j_{gy}$ just cancel, so since $\delta_1 j_{gx}$ is odd in

H, the total $j_{gx}(\mathbf{H})+j_{gx}(-\mathbf{H})$ remains zero to at least the second order in H. This is easily shown to be equivalent to saying that $\bar{Q}_g(\mathbf{H})+\bar{Q}_g(-\mathbf{H})$ is unchanged to this order.

The result (D.4) can be proved to arbitrary order by subjecting all vectors to a linear transformation which projects the tensor $\tau^{-1}\cdot\mathbf{m}^*$ into a multiple of the unit tensor. Let us use primes to denote transformed vectors. In the transformation, $\mathbf{E}$ and the $\mathbf{E}_g$ of (13) behave as covariant vectors, $\mathbf{H}$ and $\mathbf{j}_g$ as contravariant vectors. The relation of $\mathbf{j}_g'$ to $\mathbf{E}'$ and $\mathbf{H}'$ becomes isotropic. For a fixed $\mathbf{E}'+\mathbf{E}_g'$, therefore, $\mathbf{j}_g'(\mathbf{H})+\mathbf{j}_g'(-\mathbf{H})$ must by symmetry be coplanar with $\mathbf{j}_g'(0)$ and $\mathbf{H}'$. Since all the latter vectors transform in the same manner, $\mathbf{j}_g(\mathbf{H})+\mathbf{j}_g(-\mathbf{H})$ will be coplanar with $\mathbf{j}_g(0)$ and $\mathbf{H}$. If $\mathbf{E}+\mathbf{E}_g$ is such as to make $\mathbf{j}_{gx}(0)=0$, the same $\mathbf{E}+\mathbf{E}_g$ will make $\mathbf{j}_{gx}(\mathbf{H})+\mathbf{j}_{gx}(-\mathbf{H})=0$. As before, this is easily shown to imply (D.4).

PHYSICAL REVIEW VOLUME 111, NUMBER 1 JULY 1, 1958

Precipitation of Cu in Ge. II. Supersaturation Effects

A. G. TWEET
General Electric Research Laboratory, Schenectady, New York
(Received February 27, 1958)

Studies have been made on the precipitation kinetics of Cu from supersaturated solid solution in Ge crystals with dislocation densities $<100/\text{cm}^2$. We found that the precipitation rates are very strongly dependent upon the degree of supersation. We believe this is evidence for the nucleation of the precipitate particles upon a single type of nucleation site, whose identity has not been established. An attempt is made to fit the experimental data to the simple theory of nucleation in which σ, the surface tension in the phase boundary between precipitate and host lattice, and E_p, the structure-sensitive increase in strain energy in the crystal upon formation of the precipitate, are parameters. We find that the data can be fit by $\sigma\approx 500\pm 50$ ergs/cm^2, and $E_p\approx(1\pm 1)\times 10^{-13}$ erg/atom, assuming spherical precipitates. No other information about these quantities is available for comparison. An appendix gives a simplified treatment of Ham's derivation of the kinetic law for diffusion-limited precipitation upon spherical precipitate particles, which relates the observed precipitation rate to the number of precipitate particles. Theory and experiment are in reasonable agreement.

I. INTRODUCTION

RECENTLY, the author[1] has studied the kinetics of precipitation of Cu from solid solution in Ge. It was found that the precipitation rate was strongly dependent upon the dislocation density in the samples, and that it was possible to distinguish a temperature interval and range of dislocation densities (see Fig. 6 for numerical values) in which the rate-limiting step in the precipitation is believed to be the diffusion of Cu atoms to dislocations. The diffusion very probably occurs by a dissociative mechanism, which has been described by Frank and Turnbull.[2] Another range of temperature and dislocation-densities was discernible (see Fig. 6) in which the rate-limiting step in the precipitation is believed to be the rate of thermal dissociation of substitutional Cu atoms from their lattice sites to make vacancy-interstitial Cu atom pairs.

However, we noted some evidence that, at a supersaturation ratio, Σ, of greater than approximately two hundred, the precipitation rate (for temperatures above $\sim$450°C) was strongly dependent upon Σ, provided the sample had a dislocation density less than $10^4/\text{cm}^2$ or so. Such behavior is indicative of nucleation of precipitates at sites other than dislocations. The present report is the result of further experimental investigation of this phenomenon, which, to the best of the author's knowledge, has not been as clearly evident in other systems.

[1] A. G. Tweet, Phys. Rev. **106**, 221 (1957).
[2] F. C. Frank and D. Turnbull, Phys. Rev. **104**, 617 (1956).

II. EXPERIMENTAL

A. Data

Bars $\sim$0.15 cm$\times$0.25 cm$\times$2 cm were cut from Ge ingots (pulled from the melt in an atmosphere of 90% N_2, and 10% H_2) which had etch pit densities $<100/\text{cm}$.[2,3] The Cu was diffused into the samples at various temperatures for times sufficiently long to bring them within a few percent of the solubility limit,[4,5] if one assumes that the diffusion occurred entirely by the dissociative mechanism.[2,6,7] The samples were then cooled in $\sim$15 sec to room temperature. (An important point related to the initial cooling will be discussed in Sec. IIB below.) The samples were then ground and etched bright and the carrier concentration was meas-

[3] The etch pits were brought out on (111) faces with CP4. Such pits are generally believed to reveal all dislocations in Ge crystals.
[4] C. S. Fuller *et al.*, Phys. Rev. **93**, 1182 (1954).
[5] H. H. Woodbury and W. W. Tyler, Phys. Rev. **105**, 84 (1957).
[6] C. S. Fuller and J. A. Ditzenberger, J. Appl. Phys. **28**, 40 (1957).
[7] A. G. Tweet, General Electric Research Laboratory Report RL-1685 (unpublished).